Metal Nanoparticles Enhances Sorafenib Activity against Cancerous Cell Lines

By

Student Name

Muhammad Ammad Jamil

Registration No

00000401355

Department of Biomedical Engineering and Sciences

School of Mechanical and Manufacturing Engineering

National University of Science and Technology (NUST)

Islamabad, Pakistan

2024

Metal Nanoparticles Enhances Sorafenib Activity against Cancerous Cell Lines

By

Student Name

Muhammad Ammad Jamil

Registration Number

00000401355

A thesis submitted to the National University of Sciences and Technology, Islamabad,

in partial fulfillment of the requirements for the degree of

MS Biomedical Sciences

Thesis Supervisor:

Dr. Adeeb Shehzad

Department of Biomedical Engineering and Sciences

School of Mechanical and Manufacturing Engineering

National University of Science and Technology (NUST)

Islamabad, Pakistan

2024

THESIS ACCEPTANCE CERTIFICATE

THESIS ACCEPTANCE CERTIFICATE

Certified that final copy of MS/MPhil thesis written by **Regn No. 00000401355 Muhammad Ammad Jamil** of **School of Mechanical & Manufacturing Engineering (SMME)** has been vetted by undersigned, found complete in all respects as per NUST Statues/Regulations, is free of plagiarism, errors, and mistakes and is accepted as partial fulfillment for award of MS/MPhil degree. It is further certified that necessary amendments as pointed out by GEC members of the scholar have also been incorporated in the said thesis titled. **Metal Nanoparticles Enhances Sorafenib Activity Against Cancerous Cell Lines**

Signature: _____

Name (Supervisor): Adeeb Shehzad

Date: 22 - Jul - 2024

Signature (HOD): _____

Date: 22 - Jul - 2024

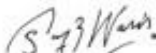Signature (DEAN): _____

Date: 22 - Jul - 2024

TH-4 Form

National University of Sciences & Technology (NUST)
MASTER'S THESIS WORK

We hereby recommend that the dissertation prepared under our supervision by: Muhammad Ammad Jamil (00000401355) Titled: Metal Nanoparticles Enhances Sorafenib Activity Against Cancerous Cell Lines be accepted in partial fulfillment of the requirements for the award of MS in Biomedical Sciences degree.

Examination Committee Members

1. Name: Muhammad Asim Waris   Signature:

2. Name: Aneeqa Noor   Signature:

3. Name: Waheed Miran   Signature:

Supervisor: Adeeb Shehzad   Signature:

Date: 22 - Jul - 2024

22 - Jul - 2024

Head of Department   Date

COUNTERSINGED

22 - Jul - 2024

Date   Dean/Principal

CERTIFICATE OF APPROVAL

This is to certify that the research work presented in this thesis, entitled "**Metal Nanoparticles Enhances Sorafenib Activity against Cancerous Cell Lines**" was conducted by **Mr. Muhammad Ammad Jamil** under the supervision of **Dr. Adeeb Shehzad.** No part of this thesis has been submitted anywhere else for any other degree. This thesis is submitted to the School of Mechanical and Manufacturing Engineering in partial fulfillment of the requirements for the degree of Master of Science in Field of Biomedical Sciences, Department of Biomedical Engineering and Sciences, National University of Sciences and Technology, Islamabad.
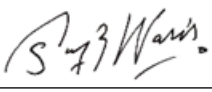
Student Name: Muhammad Ammad Jamil   Signature: _____

Supervisor Name: Dr. Adeeb Shehzad   Signature: _____

Name of Dean/HOD: Dr. Muhammad Asim Waris   Signature: _____

AUTHOR'S DECLARATION

I hereby state that my MS thesis titled "Metal Nanoparticles Enhances Sorafenib Activity against Cancerous Cell Lines" is my own work and has not been submitted previously by me for taking any degree from National University of Sciences and Technology, Islamabad or anywhere else in the country/ world.

At any time if my statement is found to be incorrect even after I graduate, the university has the right to withdraw my MS degree.

<div align="right">

Muhammad Ammad Jamil

22nd July, 2024

</div>

PLAGIARISM UNDERTAKING

I solemnly declare that research work presented in the thesis titled "Metal Nanoparticles Enhances Sorafenib Activity against Cancerous Cell Lines" is solely my research work with no significant contribution from any other person. Small contribution/ help wherever taken has been duly acknowledged and that complete thesis has been written by me.

I understand the zero tolerance policy of the HEC and National University of Sciences and Technology (NUST), Islamabad towards plagiarism. Therefore, I as an author of the above titled thesis declare that no portion of my thesis has been plagiarized and any material used as reference is properly referred/cited.

I undertake that if I am found guilty of any formal plagiarism in the above titled thesis even after award of MS degree, the University reserves the rights to withdraw/revoke my MS degree and that HEC and NUST, Islamabad has the right to publish my name on the HEC/University website on which names of students are placed who submitted plagiarized thesis.

Name: Muhammad Ammad Jamil

Student Signature:

This work is dedicated to my parents whose unwavering love and support propelled me through my academic journey. This degree is the proof of their endless sacrifices and belief in me.

<u>ACKNOWLEDGMENTS</u>

Table of Contents

List of Table

List of Figures

List of Abbreviations

Abbreviations	Definition
FBS	Fetal Bovine Serum
PBS	Phosphate Buffered Saline
DMEM	Dulbecco's Modified Eagle Media
EDTA	Ethylene Diamine Tetra-acetic Acid
MCF-7	Michigan Cancer Foundation -7
UV-spectrophotometry	Ultraviolet-visible spectrophotometry
FTIR	Fourier Transform Infrared Spectroscopy
SEM	Scanning Electron Microscopy
XRD	X-Ray Diffraction
DLS	Dynamic Light Scattering
ER	Estrogen Receptor
VEGFR	Vascular Epithelial Growth Factor Receptor
PDGFR	Platelets Derived Growth Factor Receptor
RAF	Rapid Accelerated Fibrosarcoma
MEK	Mitogen - Activated Protein Kinase
c-kit	c-proto oncogene tyrosine protein kinase kit
Flt	Fms-like tyrosine kinase
MCL-1	Myeloid Cell leukemia-1
eIF4E	Eukaryotic Translation Initiation Factor 4E
b.i.d	Bis in die (twice a day)
HT-29	Human colon adenocarcinoma
A-498	Human breast cancer
DEN	diethyl nitrosamine
Ras	Rat sarcoma
NF gene	Neurofibromatosis gene
BRAC	Breast Cancer susceptibility gene
DPC-4	Deleted in pancreatic cancer-4
APC	Adenomatous polyposis coli
PDGF	Platelets Derived Growth Factor
myc	Myelocytomatosis
MRI	Magnetic Resonance
EGD	Esophagogastroduodenoscopy
ERCP	Endoscopic Retrograde Cholangiopancreatography
ROCK	Rho-associated protein kinase
HCC	Hepatocellular carcinoma
CP	Child-Pugh
SHARP	Sorafenib hepatocellular associated randomized protocol
UGT1A9	UDP Glucuronosyltransferase Family 1 Member A9
CYP3A4	Cytochrome p450 3A4
GI	Gastrointestinal
SPC	Summary of Product Characteristics
BCLC	Barcelona Clinical Liver Cancer

HCV	Hepatitis C Virus
MVI	Microvascular Infusion
DPPH	2,2-Diphenyl-1-picrylhydrazyl
MTT	3-(4,5-Dimethylthiazol-2-yl)-2,5-diphenyltetrazolium bromide
GABA	Gamma-aminobutyric acid
NADH	Nicotinamide adenine dinucleotide
CuCl2	Copper chloride
CaCl2	Calcium chloride
ZnCl2	Zinc chloride
NaOH	Sodium hydroxide
PET	Positron emission tomography
CT	Computed tomography

ABSTRACT

Globally, cancer prevalence is increasing rapidly, requiring urgent development of effective therapeutics strategies. Cancer is characterized by uncontrolled cell growth and is categorized into various stages and types, each with different epidemiology. Cancer cell lines are derived from many tumor types, then cultured in vitro, and are essential for studying cancer genetic and drug testing. Sorafenib is a multi-kinase inhibitor drug, widely used in treatment of hepatocellular carcinoma and renal cell carcinoma, but has limitations such as low bioavailability and solubility. This study deals with the use of bacopa monnieri for the synthesis of copper formulated and zinc formulated nano-coated drugs; and investigates their effect of on cancer cell line (MCF-7). Both nano-coated drugs were characterized by various techniques; UV-Vis spectrometry confirmed the drug absorbance at 262nm and 263nm, Fourier transform infrared spectroscopy (FTIR) confirmed the presence of interaction between the sorafenib drug and nanoparticles, X-ray diffraction (XRD) confirmed their crystallinity nature, Scanning electron microscopy (SEM) revealed that copper formulated nano-coated drug was stable with good coating and surface morphology and zinc formulated nano-coated drug was less stable due to irregular shape morphology, Dynamic light scattering (DSL) confirmed that copper formulated nano-coated drug size ranged from 12nm to 13nm and zinc formulated nano-coated drug size ranged from 9nm to 10nm, Zeta potential confirmed that copper formulated nano-coated drug was stable (fit values ranged between (-21mV− -18mV)) and zinc formulated nano-coated drug was slightly less stable (fit values ranges -7.12mV− +12.35mV). MTT assay showed that copper formulated nano-coated drug has the cell viability of 64.8% with IC_{50} value of 4.599μM and zinc formulated nano-coated drug has the cell viability of 68.5% with IC_{50} value of 34.50μM. Both nano-coated drugs exhibited less cell viability than the actual drug and are stable, thus, making them suitable for the cancer treatment.

Keywords: Cancer, Cell Lines, Sorafenib, Nanoparticles, Characterization, Anti-cancer Activity

CHAPTER 1: INTRODUCTION

1.1. Cancer:

Cancer is the hallmark of versatile and complex disease that is characterized by the uncontrolled spread of aberrant cells. and It results from genetic alterations that interfere with the regular regulatory processes that control cell division and apoptosis (Miramontes *et al.*, 2018). Although these mutations are frequently caused by environmental factors such exposure to toxins, lifestyle decisions, and random cellular errors during DNA replication, they can also be inherited (Leuthner *et al.*, 2021). Over 100 distinct forms of cancer exist, with each one categorized according to the source of the aberrant cells. Examples of these include carcinomas, sarcomas, lymphomas, and leukemia. Cancer has significant health impact as it is the main cause of death and morbidity globally (Testa *et al.*, 2018). Personalized medicine and targeted therapies have been developed as a result of improvements in our understanding of cancer biology brought about by medical research advancements. The intricacy of cancer still presents major obstacles to detection, treatment, and prevention despite these breakthroughs, highlighting the need for further research and innovation in this vital area of healthcare (Caracciolo *et al.*, 2019).

1.1.1. Cancer Epidemiology:

With an expected 20 million new cases and 9.7 million cancer-related deaths reported globally in 2022, cancer continues to be a major global health concern in 2023. The aging and growing population, together with increased exposure to risk factors such physical inactivity, poor food, alcohol use, and smoking, are the main causes of the rising cancer incidence and death rates (Bray *et al.*, 2024). The most prevalent disease to be diagnosed with and the primary cause of cancer-related deaths worldwide, especially for males, is lung cancer. Lung, colorectal, and cervical cancers are the next most common causes of cancer-related deaths in women, with breast cancer continuing to be the most common disease to be diagnosed (Schwartz *et al.*, 2024). There are significant regional differences in cancer incidence and mortality, with lower-income nations having lower cancer incidence but higher death rates. Inadequate early detection and treatment services are frequently to blame for this. For example, despite a far lower incidence rate, the death rate from breast cancer in Ethiopia is twice as high as in the US (Davey *et al.*, 2021). Furthermore,

in Latin America and sub-Saharan Africa, cervical cancer continues to be the primary cause of cancer-related deaths among women (Momenimovahed *et al.*, 2023).

1.2. Cancer Cell Lines

In cancer research, cancerous cell lines are a vital resource. These are populations of cancer cells that have been cultivated from tumors, which enables safe testing outside of human tissue. They can be used to test possible therapeutic medications, examine the behavior of cancer cells, and comprehend the mechanisms underlying carcinogenesis and metastasis. They can serve as a representative example of a particular form of cancer (Jin *et al.*, 2020).

1.2.1. MCF-7 Cell Lines

MCF-7 cell lines are the most popular model used to research estrogen receptor (ER)-positive breast cancer. MCF-7 cells, which were created in the 1970s, still have progesterone and estrogen receptors, among other characteristics of breast epithelial cells. Because of this, they are especially helpful in examining the impact of anti-estrogen therapy and hormone-dependent breast malignancies (Horwitz *et al.*, 2020). Although MCF-7 cells provide insightful information, it's crucial to understand that they only represent one subtype of breast cancer and might not adequately convey the complexity of the condition (Kowalczyk *et al.*, 2021).

1.3. Sorafenib Drug

Sorafenib is a kinase inhibitor drug that is marketed under the Nexavar brand. It is a targeted therapy for a variety of advanced cancer forms. Sorafenib acts by preventing the action of particular enzymes (kinases) that are involved in the growth of tumor cells and the development of blood vessels inside tumors (Z. Cheng *et al.*, 2020). This stops cancer cells from growing and spreading. Hepatocellular carcinoma, an advanced form of kidney cancer, renal cell carcinoma, and a particular kind of thyroid cancer that is resistant to radioactive iodine therapy can all be treated with sorafenib. Sorafenib can help reduce tumor growth and increase survival rates in some cases, but it cannot cure cancer (Wang *et al.*, 2023).

1.3.1. Mechanism of action

Sorafenib act as a dual action inhibitor by targeting the tyrosine kinases VEGFR/PDGFR in the tumor metastasis and the RAF/MEK/extracellular signal regulated kinase (ERK) pathway in tumor cells. The molecular name of this orally accessible medication, 4-[4-[[4-chloro-3-(trifluoromethyl)

phenyl] carbamoyl-amino] phenoxy], belongs to a novel class of biaryl urea agents. The structure of -N-methylpyridine-2-carboxamide is displayed in Box 1 (Tang *et al*., 2020). Combinatorial and medicinal chemistry techniques were used to produce sorafenib as an inhibitor of C-RAF kinase. It was discovered to be a multi-kinase inhibitor of VEGFR-1 (IC_{50} 165 ng/ml), VEGFR-2 (IC50 570 ng/ml), VEGFR-3, platelet-derived growth factor receptor-b, c-kit, and Flt-3 in preclinical investigations (Ishihara *et al*., 2019). Different tumor types respond differently to sorafenib's anti-proliferative action, which is mostly dependent on the oncogenic signaling pathways that drive tumor growth. It was also examined that sorafenib causes apoptosis in a various tumor cell lines. A recurring motif in sorafenib-induced apoptosis is the loss of the anti-apoptotic protein myeloid cell leukemia-1 (MCL-1), as well as the inhibition of phosphorylation of the initiation factor eIF4E (Raju *et al*., 2022). The exact mechanism underlying this induction of apoptosis is not entirely understood and may differ throughout cell lines. It was recently demonstrated that sorafenib inhibits the multiplication of the hepatitis C virus in vitro, and investigations conducted in vitro have also revealed some direct effects on immune cells (Hosseinzadeh *et al*., 2022).

1.3.2. *Oral administration and Pharmacokinetics*

After reaching its peak plasma levels, sorafenib has a mean elimination half-life of around 25 to 48 hours. After 7 days, sorafenib concentrations reach steady-state levels with a peak-to-trough ratio of less than 2 (Grassin-Delyle *et al*., 2022). In comparison to the solution form, the tablet formation has mean relative bioavailability of 38–49%. Since eating a high-fat meal reduces sorafenib's bioavailability by 29%, sorafenib should be taken without meals. A single daily dose does not provide a comparable exposure as twice-day doses (Chryssafidis *et al*., 2021). Furthermore, exposure to sorafenib was dose-proportionate up to 400 mg b.i.d (means two times per day). The exposure to sorafenib increased less than dose-proportionately at dosages exceeding 400 mg b.i.d. When administered twice daily instead of as a single dosage, sorafenib levels increase 2.5–4.7 times after the prescribed 400 mg b.i.d. dose (Chen *et al*., 2020).

1.4. Bacopa monnieri

Bacopa monnieri is a member of the Scrophulariaceae family and is also known as aindri and in Sanskrit as brahmi. It is a somewhat succulent, glabrous, creeping herb that grows up to 1500 meters in altitude in the rainy regions of adjacent tropical countries and India. Because of its capacity to enhance brain function, bacopa is also referred to as medhya rasayana (Prabhuji *et al*.,

2023). All Ayurvedic practitioners use this herb extensively to treat ailments like fever, pain, inflammation, epilepsy, asthma, memory loss, and insanity. The main component responsible for these neuro-pharmacological effects is bacoside A, a triterpenoid saponin of the dammarane type whose aglycone units are either jujubogenin or pseudo-jujubogenin moieties. Bacoside A3 is the component of bacopaside A, bacopaside II, bacopaside X, and the jujubogenin isomer of bacopasaponin C (Sekhar *et al.*, 2019). Twelve of the bacoside family's analogs have been clarified based on structural similarities. Several saponin classes, known as bacopasides I–XII, have recently been identified as significant components of the herbal extract (Mundkinajeddu *et al.*, 2004). Hersaponin, apigenin, D-mannitol, cucurbitacin, monnierasides I–III, and plantainoside B have also been reported to be present in the plant, along with the alkaloids brahmine, herpestine, nicotine, and monnierin. The herb's significant concentrations of phenolic chemicals and avanoids contribute to its potent antioxidant qualities (Malhotra *et al.*, 2023).

1.4.1. *Bacopa monnieri in Cancer:*

Earlier research has revealed that B. monnieri may have anticancer properties. In MCF-7 (human breast cancer), HT-29 (human colon adenocarcinoma), and A-498 (human breast cancer) cell lines, researchers also reported the anticancer activity of bacoside A from the entire plant of B. monnieri (Ghosh *et al.*, 2021). According to Janani *et al.*, bacoside A has chemo-preventive effects on cancer produced by diethyl nitrosamine (DEN) by lowering lipid peroxidation levels and boosting antioxidant status, most likely by scavenging free radicals (Sivakumari *et al.*, 2022). In rats with 3-methylcholanthrene-induced brosarcoma, B. monnieri's antioxidant and tumor-inhibiting abilities were also documented. Supplementing with B. monnieri improved the status of antioxidant enzymes, decreased the lipid peroxidation rate, and tumor formation indicator's downregulation. Based on bioassay-guided methodologies, researchers also found that of the five crude samples, which included the whole plant of B. monnieri and four different fractions of the methanol extract, the n-butanol fraction had the strongest anticancer activity (Momtazi-Borojeni *et al.*, 2013).

1.5. Nanoparticles

Nanoparticles are (NPs) small in size, having huge surface area, surface charge and surface chemistry. Nanoparticles are an immense class of components those consists of particulate substances, having 1 dimension less than 100 nm (Laurent *et al.*, 2008). Nanoparticles, also known

as nanomaterials, are one millionth of a millimeter in size. The majority nanoparticles are excessively tiny to be seen with the naked eye or even normal laboratory microscopes. Nanoparticles can be made commencing both natural and manmade materials (Jeevanandam *et al*., 2018). Synthetically created nanoparticles have sparked considerable interest in recent years, and base on their chemical contents, nanoparticles can be generally categorized into two main classes: organic materials and inorganic materials. Liposomes, carbon emulsions, dendrimers, nanotubes and other polymers are examples of organic materials, while metals are examples of inorganic materials. 1–3 Nanoparticles of various sizes (1.0–500 nM) and morphologies can be produced (A. Khan *et al*., 2018).

1.5.1. Synthesis Methods for Nanoparticles

There are two methods for producing nanoparticles: by deriving them from bigger molecules (top down technique), and by combining lesser atoms (bottom up approach) (Thiruvengadathan *et al*., 2013).

1.5.1.1. Top-down Method

In order to produce the Nanoscale material, the substance from the mass is fixed away in the top down approach. For size reduction, a variety of physical and chemical approaches could be used. Sputtering, etching, mechanical, pulse laser ablation, milling-ball milling, discharge, lithography, pulse wire, explosion process, and evaporation condensation retort are all part of the top down technique. However, the biggest disadvantage of this process is that it introduces defects to the product's surface. This could cause problems with the product's surface chemistry and other physical qualities (Iravani *et al*., 2011).

1.5.1.2. Bottom-up Method

Single molecules organize itself through the technique of self-assembly in the bottom-up method. The product is made up of smaller things such as atoms & molecules that are bonded together. Due to the atom-by-atom type of arrangement, homogeneous assembling at the nanoscale in the material may be achieved using this method. This strategy could potentially use a variety of chemical or biological techniques, including as Sol-gel procedure, electrochemical, aerosols and sol process, hydrothermal, photocatalysis, sonochemical, chemical reductions, pyrolysis, templating, fire spraying, spinning, or green synthesizing are all examples of chemical vapor deposition (CVD) (Thakkar *et al*., 2010).

1.5.1.3. Green Synthesis of Nanoparticles

Plant extracts are employed in the plant-mediated synthesis of nanoparticles, which is another, simple, environmentally friendly, bio-reductive, and less costly method. It takes less time to react and takes place in a natural setting. The quantity of metal salts, reducing agents, and heat are all factors that impact their formation. PH and reaction time. Within 15 minutes of incubation, NPs are usually produced, and the rate of synthesis gradually rises with time. Proteolytic enzymes, carbohydrates, alkaloid, polyphenols, terpenoids, phenols, and minerals are all involved in the biomaterial reduction, synthesis, preservation, and durability of nonhazardous NPs with exceptional form and size (B. Singh *et al.*, 2016). Reducing agents often give electrons to metal ions and reduce these to Nanoparticles during the production of Nanoparticles. The Nanoparticles have a high thermal conductivity and attempt to combine against each other and the order to transition to their reduced surface energy crystal structures. As a result, the existence of additional reduction and stabilizing chemicals prevents Nanoparticles aggregation promotes the formation of smaller Nanoparticles (Shah *et al.*, 2015). Because of multiple role of plant as reducing agents, capping agents, and complexing agents, naturally occurring substances found in plants (also known as phytochemicals like polyphenols, tannins, flavonoids, alkaloids, terpenoids, and alcoholic compounds) are being more often used in the manufacture of nanomaterials. Furthermore, when compared to traditional chemical procedures, using natural agents like phytochemicals to fabricate nanomaterial is a more environmentally friendly and long-term solution (Yuliarto *et al.*, 2019).

1.6. Aims and Objectives

Aims and objective of the study are as follows:

➢ To produce Copper formulated and Zinc formulated nano-coated drugs.

➢ To characterized both nano-coated drugs.

➢ To determine its effect on the cell culture.

CHAPTER 2: LITERATURE REVIEW

2.1. Cancer

Cancer is an extensive term for diseases characterized by uncontrolled division of cells due to the cellular changes in the body. Primarily, cancer includes over 100 different diseases which develop overtime due to uncontrolled up-regulation of cells of body. It's a diseases that can originate in any tissue of body, with each type of cancer having its own unique characteristics. Cancer starts when the cell escapes the normal regulatory mechanism of division of cell and begins its own independent proliferation (Franks *et al*., 1997).

The cancer term is derived from Greek word "*Korkinoma*" which later evolved into Latin "Cancer". In 1600s (Hooke) and in 1800s (Virchow), observed that the tissues on living organisms are composed of cells and all cells are originated from other cells. This understanding resulted in the further questioning about the cancer. In 1775, notably the scrotal cancer incidence was reported among the boys working as Chimney sweeps. In Germany by mid of 1800s, the lung cancer rate among pitchblende miners was significantly higher (S. L. Jain *et al*., 2013).

Late 1900s, some physicians speculate that smoking cigars and cigarettes were closely linked with the mouth and throat cancer. These observation along with others, suggested that the cancer's origin and cause might lie outside the body, which highlights that cancer potentially linked with preventable and identifiable factors (Burnham *et al*., 1989).

In normal healthy body there are 30 trillion cells that lives in a complex were they regulates each other's proliferation. When signaled by other cells, normal cells reproduce assuring the persisted collaboration. This uncasing teamwork ensures that each tissue maintains an appropriate structure and size to meet the needs of body (Hatton *et al*., 2023). Cancer cells ignores the normal proliferation controls and executes their own reproduction agenda. Tumors made up of these malignant cells becomes progressively invasive over time and turn lethal when they interfere with the tissues and organs essential for survival for whole organism (Tarin *et al*., 2011). Scientists have identified some fundamental principles regulating the cancer development: tumor cells originates from common forebear cells that decades before tumor is detectable and starts replication inappropriately. Then malignant cells transformation occurs through the aggregation of mutations in genes within these cells (Trusolino *et al*., 2010). These genes are vital to understand the fundamental processes underlying human cancer. Genes are encoded within the DNA molecules

located in the chromosomes of nucleus of cell. Gene direct the sequence of amino acids required for the particular protein formation. This protein preform the function regulated by gene. When the activation of gene occurs the cell responds by the producing the encoded protein. Gene mutation can disrupt the cell by altering the proteins quantity and function. Two classes of gene, representing the small fraction of entire genetic set, significantly plays a vital role in the cancer initiation (Jacob *et al*., 1961).

2.1.1. *Tumor development*

Tumor development progresses through three primary stages. First, genetically altered cell begins the process when the certain cells in a normal population attains a mutation in the gene which enhances their proliferation ability even when they remain latent. The second stage, known as hyperplasia, involves the mutated cells and their progeny to look normal but demonstrating the excessive reproduction. One in a million of these cells undergo another mutation after years that relaxes the control over growth of cell. Dysplasia is the final stage, characterized by offspring cell appearing abnormal in alignment and shape. The tissue is said to be dysplastic. Once again, over the time a rare mutations occurs that further changes the behavior of cell (Sarkar *et al*., 2013). After these initial stages, cancer or in-situ cancer, development begins in the fourth stage where the affected cells exhibit even more abnormal shape and growth. If the tumor remain confined and doesn't metastasis to other tissues, it is known as in-situ cancer. This tumor may remain confined permanently; however, over the time, some cells may attain further mutations (Klein *et al*., 2013). In fifth stage, if the changes in genetic allows the tumor to metastasis to other tissues and release cells into lymph or blood, the mass become malignant. In body, these rogue cells can establish new tumors, potentially becoming lethal by disturbing the essential organs of body (Jones *et al*., 2024).

2.1.2. *Genes Involve in Human Cancers:*

Proto-oncogenes are genes that direct the proteins responsible for the cell division stimulation. These genes become oncogenes when they get mutated, leading to hyperactive stimulatory proteins and resulting in uncontrolled cell proliferation. Alternatively, cell division is inhibited by proteins produced by tumor suppressor genes. Mutations in these genes can inactivates the proteins,

abolishing the vital cell growth controls. Researchers are still investigating to understand the specific roles of many tumor suppressor genes (Das *et al.*, 2020).

Table 2.1: Some Tumor Suppressor Genes

Genes	Involved in	References
APC	Involved in Stomach and Colon Cancer.	(Yen *et al.*, 2022)
DPC 4	Involved in Pancreatic Cancer.	(Chai *et al.*, 2024)
WT 1	Involved in Tumor of Kidney.	(Ferrari *et al.*, 2023)
MTS 1	Involved in board range of cancer.	(Talukder *et al.*, 2021)
NF-1	Involved in Peripheral Nervous System Cancer.	(Tamura *et al.*, 2021)
NF-2	Involved in Brain Cancer	(Tamura *et al.*, 2021)
BRAC 1,2	Involved in Breast Cancer.	(Pujol *et al.*, 2021)

Table 2.2: Some Oncogenes

Genes	Involved in	References
PDGF	Involved in Brain Cancer.	(Guérit *et al.*, 2021)
Ki-Ras	Involved in Ovarian Cancer, lung Cancer, Pancreatic Cancer and Colon Cancer.	(McCormick, 2022)
N-Ras	Involved in Leukemia	(Ney *et al.*, 2021)
C-myc, L-myc, N-myc	Involved in Breast Cancer, Leukemia, Lung Cancer, Stomach Cancer and Nerve Cell Cancer.	(Duffy *et al.*, 2021)
RET	Involved in Thyroid Cancer.	(Santoro *et al.*, 2020)

2.1.3. Categories of Cancer:

There are five categories which suggests blood and tissue classification of cancer.

2.1.3.1. Carcinoma

Cancer which covers the surfaces of glands, organs, and body structure, and found in epithelial tissue is referred as carcinoma. There are four main carcinomas types: Merkel

cell carcinoma, melanoma, basal cell carcinoma, and squamous cell skin cancer (Walsh *et al.*, 2021).

2.1.3.2.   Sarcoma

This malignant tumor originates in connective tissues such as fat, muscles, cartilage, bones and tendons. These are most frequently involves in bone such as chondrosarcoma (involved in cartilage) and osteosarcoma (involved in bones). Sarcoma have four types: osteosarcoma, soft tissue sarcoma, Ewing's sarcoma, and chondrosarcoma (Rinke *et al.*, 2024).

2.1.3.3.   Myeloma

It develop within the plasma cells of the bone marrow. In certain instances, these myeloma cells are known as plasmacytoma by forming the solitary tumor gathering cells in a single bone. Alternatively, in other cases, myeloma cells are known as multiple myeloma, when these cells gather in multiple bones, resulting in several bone tumors (Cowan *et al.*, 2022).

2.1.3.4.   Lymphoma

Originates in nodes or glands of lymphatic system. It includes three types: cutaneous lymphoma, Hodgkin's and Non-Hodgkin's lymphoma (Lewis *et al.*, 2020).

2.1.3.5.   Leukemia

It is known as blood cancer. This condition alters red blood cells, white blood cells and platelets normal production. Leukemia types includes: Acute myeloid leukemia, chronic myeloid leukemia, Agnogenic myeloid leukemia, acute lymphocytic leukemia, Hairy cell leukemia, Myelodysplastic syndromes, and Essential thrombocythemia (Pelcovits *et al.*, 2020).

2.1.4.   Cancer Types

Cancer is a group of diseases which causes the body cells to grow abnormally. Each cancer types basically named after the particular part of body from where it's originates. Some cancer types are as follows:

Thyroid cancer, Breast cancer, Skin cancer, Colon and Rectal cancer, Pancreatic cancer, Non-Hodgkin lymphoma, Lung cancer, Liver cancer, Prostate cancer, Melanoma, Leukemia, and many other (Farshi *et al.*, 2024).

2.1.5. Causes of Cancer

Researchers believes that cancer is not a single cause but it is cause due interaction of multiple factors together. These factors can be genetic, environmental, and others. The overall five-year survival rate for childhood cancer is approximately 80% and 68% for adults (Hill *et al.*, 2019). Researchers identify numerous frequent risk factors or exposure which includes:

2.1.5.1. Genetic Disorders

Beckwith-Wiedemann and Wiskott-Aldrich syndromes are known to affect the immune system. Another theory suggests that when stem cells in bone marrow damaged, they replicate abnormally and produce abnormal cells, which are known as cancer cells (Enteropathica *et al.*, 2017).

2.1.5.2. Family history and Inheritance

May also play a vital role in childhood cancer (Yun *et al.*, 2017).

2.1.5.3. Lifestyle Factors

Such as high-fat diet, exposure to some toxic chemicals, and smoking can be risk factors for some adult cancers (Lewandowska *et al.*, 2018).

2.1.6. Diagnosis of Cancer

There isn't a single diagnosis of cancer, multiple tests are required to determine if person have cancer or other conditions are stimulation the cancer symptoms. A patient's thorough evaluation along with diagnostic testing is required which includes its medical history, physical examination (Walter *et al.*, 2001). For diagnosis, effective testing including monitoring of disease and effective plan for its treatment is used to confirm the elimination of disease. For cancer diagnosis, procedures involves laboratory test, imaging, surgery, tumor biopsies, genetic testing, and endoscopic examinations (Raab *et al.*, 2010). To analyze the chemical components in fluids of body, common tests like blood test (CBC), tumor markers, and urinalysis is done. X-rays, bone scans, mammograms, lymphangiograms, and computed tomography (CT) are used for diagnostic

imaging, Magnetic resonance (MRI), ultrasound are also used for reflection imaging (Milevoj Kopcinovic *et al.*, 2020). Furthermore, there are various endoscopic examinations types which are employed to diagnose cancer, such as colonoscopy, sigmoidoscopy, esophagogastroduodenoscopy (EGD), cystoscopy, and endoscopic retrograde cholangiopancreatography (ERCP) (Abad *et al.*, 2022). There are various types of tumor biopsy is used for cancer diagnosis. Biopsy is the procedure in which cells or tissues is removed from the body and examined under the microscope. Several biopsies are performed in the hospitals in which anesthesia is used to numb the area, whereas some don't require any sedation (Moran *et al.*, 2013). Biopsies are done to determine to identify the cause of infection and inflammation and also to check if the tumor is cancerous or not. Common biopsies types include incisional or excisional biopsy, bone marrow biopsy, shave biopsy, endoscopic biopsy, skin biopsy, punch biopsy, and fine needle aspiration biopsy (Deshpande *et al.*, 2018).

2.1.7. *Cancer treatment*

The treatment of cancer is dependent on each patient's medical history, condition, and cancer type. Radiotherapy and chemotherapy along with biological therapies and surgery are being used to treat the cancer (Zugazagoitia *et al.*, 2016). The following are the key terms used in treating the cancer:

2.1.7.1.   Combined modality therapy

When doctors opt for multiple therapy in patient's care, such as combination of radiotherapy and chemotherapy (Mierzwa *et al.*, 2010).

2.1.7.2.   Neoadjuvant therapy

When doctors opt for multiple therapy for patient's treatment. It is used to neutralize the cancerous cells and enhances the primary therapy effectiveness (Trimble *et al.*, 1993).

2.1.7.3.   Adjuvant therapy

It is the addition treatment which may be prescribed after the primary cancer treatment completion to enhance the cure chances. For example, patients sometimes may receive multiple treatment in succession (Midgley *et al.*, 2000).

The most common treatment of cancers are:

2.1.7.4. Chemotherapy

Nowadays, it is the most common type of cancer treatment. In this the anticancer agents are used to kill or damage the cancerous cells and reducing its spread to other body parts. It also has many side effect like fatigue, hairs loss, feeling being sick, skin and nail change, problems with memory and concentration, sex and fertility issues, infectious, anemia, sore mouth, diarrhea etc. (Behranvand *et al.*, 2022).

2.1.7.5. Radiotherapy

In this radio rays are used to kill or damage the cancerous cells, non-cancerous diseases, tumors. It also have side effects like loss of appetite, fatigue, skin redness, hair loss, nausea and vomiting etc. (Chandra *et al.*, 2021).

2.1.7.6. Immunotherapy

It's also known as biological therapy or biotherapy. It is used to enhance the immune system of body or for the cancer elimination. The immune cells, antibodies and organs works together to protect and defend the body against foreign pathogens. Scientists and researchers have detected that immune system and evaluate the cancerous cells and healthy cells difference inside the body, and kill cancerous cells (Tan *et al.*, 2020).

2.1.7.7. Hormone therapy

This therapy is used to prevent and stop the tumor growth by using the supplementary hormones. This therapy depends on factors like tumor size and type, patient age and several other factors (Pinkerton *et al.*, 2020).

2.1.7.8. Bone marrow and blood therapy

This is the type of therapy in which the unhealthy bone marrow from the patient body is removed and healthy bone marrow is transferred (King *et al.*, 2018).

2.1.7.9. Angiogenesis therapy

In this therapy the inhibitors are used to prevent the growth of new blood vessel formation. These blood vessel are needed for tumor growth (Kubota *et al.*, 2012).

2.1.8. Cancer Epidemiology

2.1.8.1.   Global Burden of Cancer:

According to World Health Organization (WHO) in 2022, 20 million new cancer cases were estimated and 9.7 million deaths. Within 5 years, 53.5 million people were alive who were diagnose with cancer. About 1 people develop cancer from 5 in their lifetime, roughly 1 in 12 women and 1 in 9 men die from the cancer (Bray *et al*., 2024).

According to Data covered from 185 countries and 36 different types of cancer; lung cancer, breast cancer, and colorectal cancer were the top three majorly occurring types of cancer. Lung cancer ranked the first with 2.5 million new cases were reported and 1.8 million death cases. Breast cancer ranked the second with 2.3 million new cases reported and 670,000 death cases. Colorectal cancer ranked the third with 1.9 million new cases reported and 900,000 death cases (Bray *et al*., 2024).

For both sexes globally, there are some differences in incidence by sex and mortality. For men, mostly diagnosed cancer and most cause of death was lung cancer, for women it was breast cancer (Jemal *et al*., 2011).

For men, the second and third mostly occurring cause of cancer were the prostate and colorectal cancer, liver and colorectal cancers were the second and third cause of cancer death. For women, breast and lung cancers were the first and second for both reported cases and death (Bray *et al*., 2024).
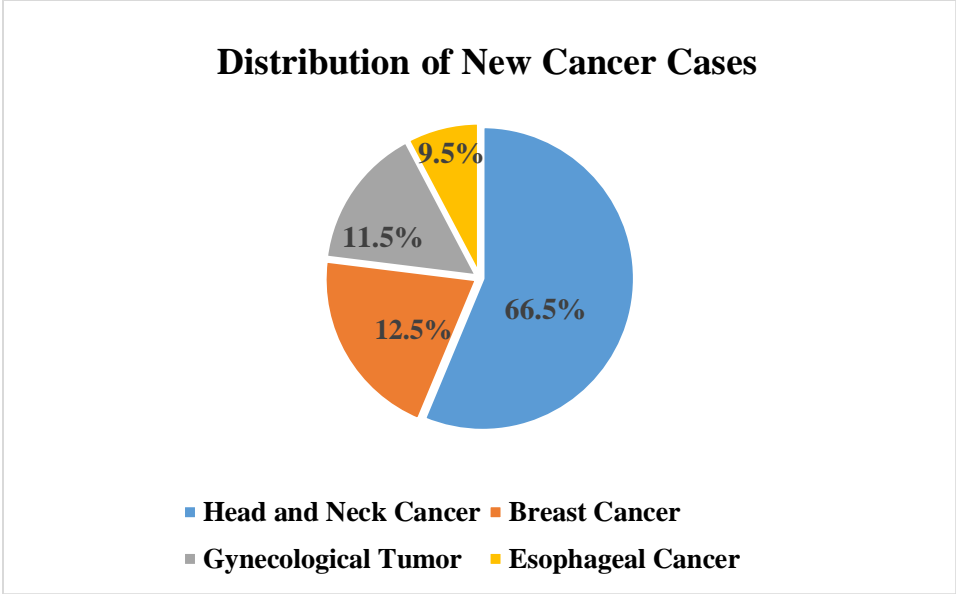
Figure 2.1: Distribution of New Cancer Cases
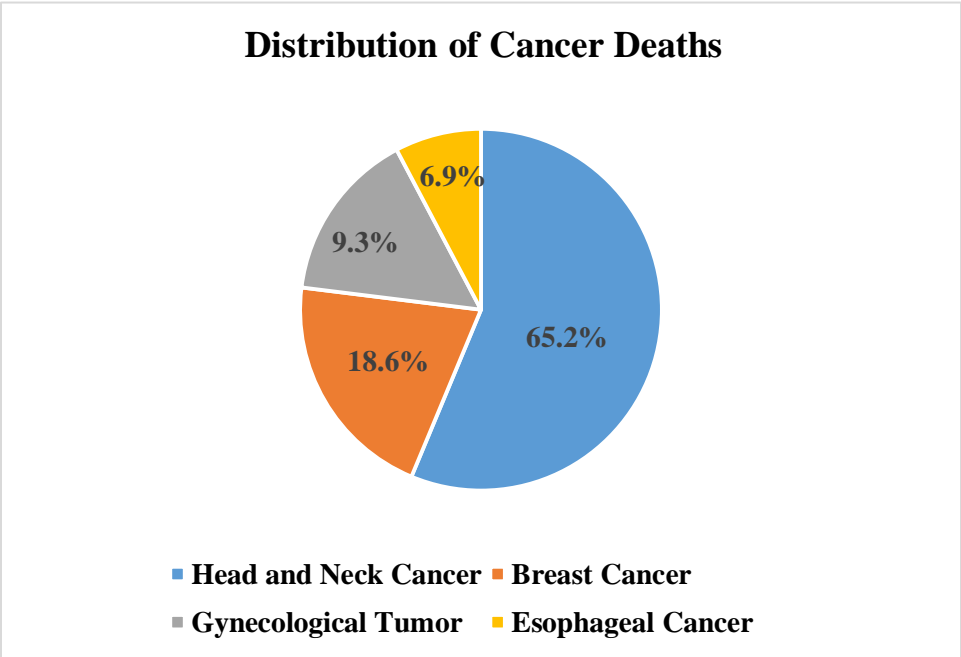
Figure 2.2: Distribution of Cancer Deaths

2.1.8.2.   Pakistan Distribution

According to the study in 2022 done in NIMRA cancer hospital in Sindh, Pakistan, seven years of cancer registry data was analyzed to check the prevalence of cancer. Total 16,191 patients were registered. For men, the mostly diagnosed types of cancer were lung, liver, colorectal, urinary tract,

and head and neck cancer. For women, most frequently diagnosed types were breast cancer, gynecological tumors, head and neck cancer, colorectal cancer, and esophageal cancer. The most leading malignant type was head and neck cancer with 37.76%, followed by breast cancer with 13.83%, gynecological tumors with10.22%, esophageal cancer with 5.18% lung cancer with 4.79% and so on (Ali *et al*., 2023).
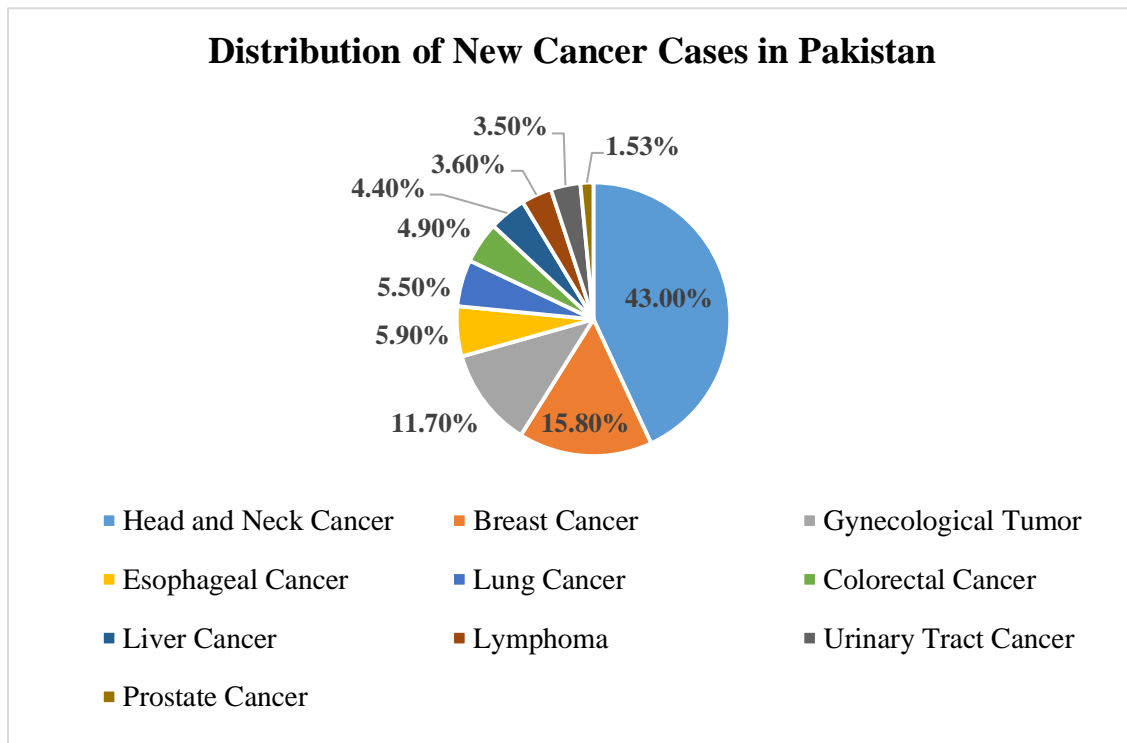
Figure 2.3: Distribution of New Cancer Cases in Pakistan

2.1.9. *Cancer Formation Mechanism*

Cancer formation is also known as carcinogenesis. The formation involve multistep through which the normal cells became malignant cells. This transformation starts when the normal regulation of cell division and growth is disrupted due to genetic mutations. These mutations can occurs through various factors such as carcinogens (chemicals or radiations), from genetic susceptibility passed from parents, or DNA replication errors. Oncogenes are the key genes involved in the cancer formation (Devi *et al*., 2004). These genes upon getting mutated or overexpressed promotes the uncontrolled proliferation of cells, and inactivates the tumor suppressor genes. Tumor suppressor genes are the genes that promote the apoptosis to inhibit the uncontrolled cell growth (Vineis *et*

al., 2010). Upon the inactivation of these genes cells can escapes the apoptosis and continue to grow abnormally. Furthermore, the tumor microenvironment plays a vital role in progression of cancer, involving the interactions with surrounding stromal cells, blood vessels, and immune system. These complex interactions leads to the abnormal cells mass formation that can invade surrounding tissues and metastasize to different body parts (Weinberg *et al*., 1996).
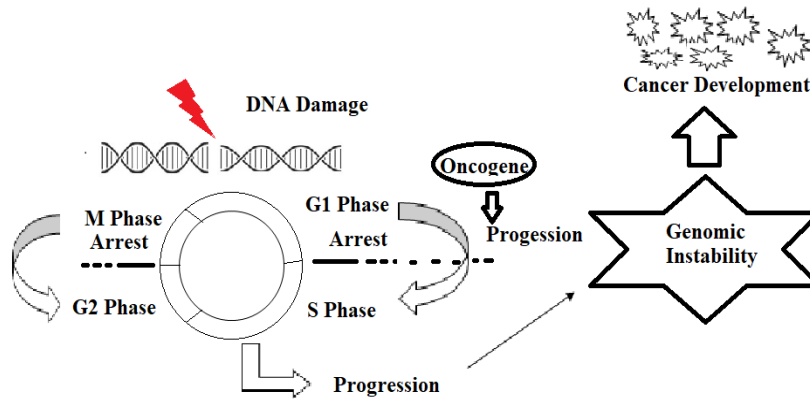
Figure 2.4: Development of Cancer

2.2.   Human Cancer Cell Lines

In recent times, human cancer cell lines are becoming a beneficial tool in the research of cancer biology. These cell lines are derived from human, these have the ability to continuously proliferate due to mutations invading cellular aging. Cell lines provides the practical model for cancer biology study and evaluating the many anticancer drugs (natural or synthetic) effectiveness (Klijn *et al*., 2015).

In cancer chemotherapy, drug resistance presents a significant challenge. Cell line studies act as an initial platform for screening to identify agents that can regulate resistance of drug. Additionally, they contribute to develop more advance models of drug resistance and examining the potential differences among drug resistant subtypes selected by different treatment protocols (PR Xavier *et al*., 2016).

2.2.1. Cancer Cell Lines

Cell lines obtained from tumors provides a controlled and condensed environment for tumor cells investigation. Cancer cell line utilization over animal model have unique advantages and disadvantages. These then determine the design of experiments (Infanger *et al.*, 2013).

One of the major advantage of using cell lines over animal models is the significantly lower cost of maintenance. Other advantages include the readily availability which allows that quick execution of research studies. Cell lines are flexible means they support the variety of studies types both xenograft model in mice to study the progression of cancer and also in-vitro studies. Over time, these can also be used to monitor sequential events in response to specific stimuli, their secretome (rich and complex structure of molecules released by living cells) can be analyzed (Wilding & Bodmer, 2014).

Along with the advantage, cell lines also have some disadvantage, as they don't fully represent the heterogeneity in the tumor microenvironment. Therefore, sometime multiple cell lines are used to observe the full spectrum of tumor phenotypes. Other disadvantage is that, over prolong experiments, during culture genetic alterations can alters the cell lines phenotypes which potentially hides insights into tumor progression and primary pathogenic pathways (Goodspeed *et al.*, 2016).

Cell lines applications in different cancer types affecting the major organs such as prostate, lung, colorectal, breast, and liver. Few are discussed below.

Table 2.3: Cancerous part and their available cell lines

Cancerous organs	Cell Lines	References
Lung Cancer	NSCLC (Non-Small Cell Lung Cancer), NLC-H125, -H157, -H226, -H358, -H661	(Gazdar *et al*., 2010)
Breast Cancer	MCF-7, MDA-MB-435	(Dai *et al*., 2017)
Colorectal Cancer	HT-29, RKO, Caco-2, HCT-116, Colo205	(Mouradov *et al*., 2014)
Liver Cancer	BEL-7402, HepG2, HuH7, hepaRG, SK-hep-1, hep3B	(Saied *et al*., 1998)
Prostate Cancer	LNCaP, LAPC-4, 9, VCaP, MDA-PCa 2a/2b, RC-77T/E.	(Russell *et al*., 2003)
Brain Cancer	U87 (Glioma cell line)	(Sedeky *et al*., 2018)
Gastric Cancer	GC1401, GC1415, GC1436, MKN28, KATOIII	(Basque *et al*., 2001)

2.2.2. *Importance of Primary Cell Culture*

Primary cell culture is the process in which a tissue maintained in a suitable medium to promote division of cell after the removal from organism. There are different methods to culture cell; one in which tissue is placed in a plastic vessel or glass and then soaked in a medium, where cell grows and divides after detaching from tissue. Another method involve the enzymes use to digest the compounds attach to cells, releasing single cells that are then cultured in medium (Kartsogiannis *et al*., 2004).

Fresh surgical dissected tissue is used to create population of ex vivo cells, for primary cancer cell culture. For studying cancer, the most widely used method involve the use of immortalized cell

lines. The questions about the accuracy of these models in representing actual behavior of cancer rises due to this transformation process (Richter *et al*., 2021).

Primary cancer cell cultures act as a vital tool for preclinical and clinical analysis as they closely reflects the behavior and phenotype of cancer tissues. To study cancer, cell lines appropriate systems by providing the maintained genetic and molecular features, storage, management and usage ease, less cost, and can easily amplified (Lv *et al*., 2017).

Single tumors can be created from primary culture which allows comparative analyses between lesions in same or different body parts. In 2008, Daigeler and his colleagues, treated that 19 liposarcoma primary culture with doxorubicin to check their degree of response at different stages of disease. They observed the same clinical degree response for different stages of disease. This shows the primary culture suitability to analyze the drug effectiveness on patients. Thus, therefore the primary cultures offers a vital tool which continue to offer the insight on cancer (Daigeler *et al*., 2009).

2.2.3. Advancement in Cell Line Development

Regardless of cell line model importance, isolating new cell lines from indolent or less aggressive tumor have low success rate. Therefore, the disease spectrum for many types of tumors is not accurately represented in the cell lines. Despite the low success rates. Researchers are interested in developing method to enhance cell lines ability (Lai *et al*., 2013). In recent time, several new methods have been developed, these are given below:

2.2.3.1.   Feeder Cell Approach

In this approach, they uses the nondividing irradiated fibroblasts of mouse to extend the lifespan of primary cells. Recently, Dr. Schlegel's lab optimized these cells by combining them with ROCK inhibitor (Y-27632) to create epithelial cell lines from numerous tumors, this approach was rapid (2 days) and have high success rate). Along with advantages like generating new cell lines with low-passage, and improved microenvironment representation of patient-derived fibroblast, this approach also have limitations like incomplete understanding of effect of ROCK inhibitor on patients (Llames *et al*., 2015).

2.2.3.2.   Xenotransplantation Approach

Since 1970s, the study of cancer utilizes the transplantation of human tumors into xenografts (immunocompromised mice). Researched examined this technique to improve the cancer cell lines colon formation. They engrafted the tumor in mice before cell culturing, and achieved 7% success rate compared to 9.7% rate using direct culturing. Notably, it is harder to establish cell lines from metastases directly in vitro. While, these xenograft-derived cell lines illustrate similar expression of gene and morphology, they differ in chromosome composition, drugs responses, and growth rate. This approach holds a promise for cultivating cell lines from challenging tumors, however its success depends on type of tumor (Cozzi *et al*., 2005).

2.2.3.3.   Chemically Defined Media Approach

Culturing cell lines is difficult due to it slow growth rate initial. Traditional methods takes month, leading to aberrant sub-clones. New approaches like feeder cells yield faster growth, but have limitation of cell properties and downstream experiments. Another new advance approach was developed, in which optimized chemical defined media is used to culture the cell lines. Using this approach, successful group of ovarian cancer cell lines were yielded with minimal changes and faster growth rate. This approach offers the cultured cell lines having close matching with original tumors. However, this approach is not universally applicable, but using this approach researchers can culture cell lines which reflects their origin accurately (Summers *et al*., 2003).

2.3.   Sorafenib

Nowadays, the sole systemic treatment licensed in order to treat HCC, or hepatocellular carcinoma is sorafenib (Nexavar®). Predicted on the crucial Asia-Pacific (AP) Sorafenib and SHARP studies, which comprised Class Child-Pugh (CP) A high grade HCC patient demonstrated no noteworthy differences in the median intervals between groups for the time to symptomatic progression (TTSP), it was approved (Mazzoccoli *et al*., 2016). Additionally, these trials demonstrated that 400 mg of sorafenib twice a day resulted in considerably extended median when as opposed to placebo, overall survival (also known as OS) and time to radiographic progression (also called TTP). Even in individuals who were specifically selected to be in the CP class B, sorafenib usage in HCC is supported by later findings from practical research like GIDEON, despite the fact that median overall survival (OS) in these patients appeared to be quite poor (Galle *et al*., 2021). There

are ways to manage and prevent side effects like hand-foot skin reactions, and sorafenib's safety and tolerability profile have been thoroughly studied. In summary, sorafenib remains a useful treatment option for HCC (Leowattana *et al*., 2023).

2.3.1. *Mechanism of Sorafenib*

Oral sorafenib is an inhibitor of several kinases. It inhibits a wide range of cytoplasmic serine or threonine kinases in the MAPK chain, such as wild-type, mutant BRAF and CRAF (Raf-1) as well as numerous tyrosine kinases on the cell surface, such as VEGFR-1 (vascular endothelial growth factor receptor), platelet-derived growth factor receptor (PDGFR)-β, VEGFR-2, and VEGFR-3. Angiogenesis, apoptosis, proliferation, and signaling from tumor cells are all impacted by these kinases (Cervello *et al*., 2012). In vitro, sorafenib accelerated apoptosis and inhibited HCC cell growth. It also inhibited the growth of tumors, promoted apoptosis in tumor cells, and decreased tumor angiogenesis in HCC models involving animals. As many other tyrosine kinase inhibitors (TKIs) did not demonstrate effectiveness in HCC, it is possible that sorafenib's action is mediated by mechanisms other than kinase inhibition (Coriat *et al*., 2012). Hsu *et al*. analyzed a number of research that looked into sorafenib's possible additional mechanisms of action. Briefly put, sorafenib impacts multiple cell signaling pathways beyond as this is important because several other cell signaling pathways (PI3K or Akt or mTOR, JAK or STAT, Wnt or β-catenin, cMET, and IGF pathways, among others) are influenced by the MAPK pathway (e.g., suppressing p-STAT3),are linked to the start and development of HCC (Hsu *et al*., 2014). By a variety of MAPK-independent ways, sorafenib also causes the death of tumor cells. These mechanisms include the p53-upregulated modulator-of-apoptosis (PUMA) being increased and the reduction of Bcl-2 anti-apoptotic proteins like Mcl-1. Additionally, sorafenib may have immunomodulatory effects, maybe by decreasing numbers of suppressive immune cells and increasing effects of effector T cell activation specific to tumors. Sorafenib-using patients typically experience medication resistance with time. Since the processes underlying the development of sorafenib resistance are complicated, it is unclear how resistance is acquired (Hasan *et al*., 2022). Potential mechanisms encompass changes in the tumor ecology with regard to angiogenesis, swelling, epithelial-mesenchymal conversions; Oxidative stress syndrome, autophagy, oxygen deprivation, inflammation, and the start of a pathway that avoids the MAPK pathway, such as the PI3K or Akt or mTOR one (Hasan *et al*., 2022).

2.3.2. Administration of Sorafenib

The average proportion of bioavailability of sorafenib in an oral solution was 38–49%; nevertheless, sorafenib tablets demonstrated a similar profile. One could reach a steady state after seven days after starting sorafenib orally, with a peak plasma concentration occurring in about three hours (Song *et al.*, 2021). As compared to fasting, sorafenib's bioavailability was 29% reduced when consumed with a meal heavy in fat. In vitro, 99.5% of the time, sorafenib linked to plasma proteins. Because UGT1A9 glucuronidates sorafenib, CYP3A4 is responsible for its oxidative metabolism. Breaking down sorafenib conjugates can help with the reabsorption of the unconjugated active ingredient in the GI tract due to the bacterial glucuronidase activity present in the GI tract. When the drug was at steady state, Nine to sixteen percent of the circulating analytes in plasma were the pyridine N-oxide metabolic product, which had sorafenib-like activity in vitro, and seventy to eighty-five percent were the parent drug (Tlemsani *et al.*, 2015). Nineteen percent of the dose of radiolabeled sorafenib was eliminated in urine, mostly as glucuronidated metabolites, and seventy-seven percent was eliminated in faeces. Five sources reported that the parent substance was found in feces only, not in pee, and accounted for 51% of the dose. Approximately 25–48 hours was the typical eradication half-life of sorafenib. When it came to sorafenib pharmacokinetics, gender, age, bodyweight, and race had no clinically meaningful impact (L. Jain *et al.*, 2009). There was no clinically meaningful change in Child-Pugh (also known as CP) class A or B individuals with light to serious liver damage or mild, moderate, or severe kidney damage in the pharmacokinetics of sorafenib, and dosage modification is not required. When individuals have substantial liver damage (CP class C) and dialysis patients, there is a dearth of information. It is best to avoid coadministration of strong CYP3A4 inducers include phenobarbital, carbamazepine, dexamethasone, and hypericum (St. John's wort), phenytoin, rifampicin, and rifabutin as these may reduce sorafenib exposure. For medications that are mostly metabolized or removed by UGT1A1 (such as irinotecan) or UGT1A9, the EU's SPC, or summary of product characteristics advises using precautions while collaborating with sorafenib. When coadministering sorafenib and docetaxel, the EU SPC advises caution as well (Thomas-Schoemann *et al.*, 2014). A 54% decrease in the mean bioavailability of sorafenib was seen upon coadministration of neomycin, an antibiotic that prevents bacterial glucuronidases in the GI tract from cleaving sorafenib conjugates. Sorafenib pharmacokinetics have not been examined in relation to other antibacterial. Before beginning antimicrobial therapy, the EU SPC advises taking

into account the possibility of decreased sorafenib plasma concentrations. The simultaneous use of omeprazole, a proton pump inhibitor, did not significantly change sorafenib's exposure, despite the fact that sorafenib's hydrolysis is pH dependent (Tuccitto *et al.*, 2018).

2.3.3. Treatment Using Sorafenib

The global, phase 3 Asia-Pacific (also called AP) for Sorafenib and SHARP studies demonstrated Sorafenib's effectiveness in addressing advanced HCC. The trials were double-blinded, randomized, and placebo-controlled. Individuals with detectable advanced HCC who were in CP class A, had not undergone systemic therapy previously, and were anticipated to have a 0–2 Eastern Co-operative Oncology Group (ECOG) efficacy prestige to live for minimum 12 weeks, with proper renal, hepatic, and haematological function (Kaseb *et al.*, 2013). Both Sorafenib AP and SHARP were carried out in Europe, Australasia, and America, as well as South Korea, China, and Taiwan (Keating *et al.*, 2017). Treatment of Sorafenib continued until the illness progressed, unacceptable side effects occurred, or other criteria for halting therapy were reached (for example, death in the case of Sorafenib AP). Treatment in SHARP was extended until both evident progression as determined by the FHSI-8 questionnaire, which is part of the Functional Assessment of Cancer Therapy] and radiographic progression [evaluated by RECIST criteria] had taken place (Azim *et al.*, 2018). At baseline, 97% of patients in both studies were termed as CP class A, and 3% as CP class B. 54, 38, and 8% of patients in SHARP and 26, 69, and 5% of individuals in The ECOG efficiency status of sorafenib AP was either 0, 1, or 2. When the patients were first diagnosed, seventeen percent of patients had stage B liver cancer (BCLC) in the Barcelona Clinic, eighty-three percent had stage C BCLC in SHARP, and ninety-six percent had stage C BCLC in Sorafenib AP. Furthermore, 21% and 32% lung involvement was present in 50% of individuals with Sorafenib AP and SHARP patients, while 26% and 50%, respectively, had lymph node involvement (McNamara *et al.*, 2018). Total The duration of OS and the onset of symptoms (TTSP; described as a drop in the rating on the FHSI8 survey from a baseline of ≥4 points, verified three weeks later, worsening to an ECOG activity level of 4, or fatality) were co-primary outcomes in SHARP. In Sorafenib AP, there was no defined primary endpoint. The population under treatment (ITT) was used to evaluate efficacy (Keating *et al.*, 2017). As of survival benefit shown with sorafenib compared to placebo at this time point, the SHARP case was stopped following the second preliminary examination. The OS of both the Sorafenib AP and

SHARP trials was significantly extended by sorafenib. Although there was no notable variation in average duration to radiographic advancement (TTP) between individuals on sorafenib and those on placebo, there was a noteworthy difference in the median TTSP. In each of the two trials, sorafenib significantly improved the disease control rate compared to placebo. A preliminary subgroup examination of the SHARP experiment revealed that there was a general consistency in the implications of sorafenib over control comparing the results of the major experiment with those on the disorder's control rate (A.-L. Cheng *et al*., 2012). Overall survival, and Time to radiographic Progression conducted over a number various subtypes, such as the origins of HCC [beneficial for both the antibodies against HCV and the surface antigen associated with hepatitis B (HBsAg)], alcohol-related; tumor pressure [extrahepatic spread (EHS) and macrovascular invasion (MVI) both absent, both present, or absent], tumor stage (BCLC B or C), tumor performance status (ECOG level of performance 0 or 1-2), and previous medication [trans-arterial chemoembolization (TACE) or preceding curable therapy]. Hazard ratios (HRs) for OS and TTP varied among the subgroups, with patients not included who tested HBsAg positivity (HR for Time to radiographic Progression of 1.03), which ranged from 0.50 to 0.85 and 0.40 to 0.64, respectively (Llovet *et al*., 2007). The Sorafenib AP trial's subgroup analysis revealed the positive implications of sorafenib compared to control on Overall survival, and Time to radiographic Progression were mostly in line with that observed in the primary trial throughout a number of small groups, such as HBV (positive or negative), the extent of tumor (either or additionally MVI and EHS existent), performance rating (ECOG outcome prestige 0 or 1-2), history of trans-arterial engorgement (TACE) and liver transplantation (yes or no), metastatic lymph node disease (yes or no), pulmonary metastasis (yes or no), and the amount of aminotransferase (regular, slightly or moderately elevated) also need to be considered, α-fetoprotein (AFP; regular or increased), and bilirubin rate (normal or increased). The range of HRs for OS and TTP across the different subgroups was 0.32 to 0.94 and 0.31 to 0.75, respectively (A.-L. Cheng *et al*., 2012). AFP level, BCLC stage, tumor pressure, tumor mass, ECOG activity status, Albumin-Bilirubin (ALBI) rate, neutrophil: lymphocyte proportion (NLR), and SHARP and Sorafenib AP trials were all found to be OS predictive variables in patients receiving sorafenib and placebo, according to a pooled analysis of these trials (available as an abstract and slide presentation) (Ogle *et al*., 2017). Not found to be predictive of OS were race (between Asians and non-Asians) or aetiology. Considering potential predictors, the advantages of sorafenib over placebo on overall survival (OS) were largely

consistent, comprising 0.47 to 0.85 for OS HRs, regardless of the individual's demographics, baseline characteristics, or prognostic variables. Nevertheless individuals infected with HCV (connection p value is 0.035), minimal EHS (p value for association = 0.015), reduced tumor pressure (p value of association 0.081) and reduced NLR (p value of association 0.05) seemed to benefit more from the treatment. When comparing individuals with high compared to average amounts of aminotransferases, AFP, or bilirubin who were getting sorafenib or a control drug, a further investigation of the SHARP case records revealed that benefit the sorafenib over controlled drug was still evident, in general, the disease control rate seemed statistically lower and the average intervals of OS and TTP appeared quantitatively shorter (Nojiri *et al.*, 2013).

2.4.   Bacopa Monnieri

The plant Bacopa monnieri belongs to the Scrophulariaceae family, is also referred to as aindri and brahmi in Sanskrit. This herb, which is glabrous and somewhat succulent, grows up to 1500 meters high in moist regions of adjacent tropical countries and India. Due to its capacity to enhance brain function, Bacopa is also referred to as medhya rasayana (Abdul Manap *et al.*, 2019). This plant is widely used by all Ayurvedic practitioners to cure a wide range of conditions, such as a high temperature, pain, swelling, allergies and asthma, epileptic seizures, insane behavior, and loss of memory. The primary chemical agent accountable for Bacoside A has these neuro-pharmacological actions. A triterpenoid saponin of the dammarane type having as its aglycone components jujubogenin or pseudo-jujubogenin moieties. Bacopaside A3, the jujubogenin isomer of bacopasaponin C, bacopaside II, or bacopaside X make up bacoside A (Ganjewala *et al.*, 2011). Twelve analogs belonging to the bacoside family are clarified according to their structural similarities. Bacopasides I–XII are the names of many saponin groups that have lately been found to be important constituents of the herbal extract. There have also been reports of the plant containing the alkaloids brahmine, herpestine, nicotine, and monnierin. The herb's significant avanoids and phenolic component content contribute to its potent antioxidant qualities (Vishnupriya *et al.*, 2017).

DNA damage can be prevented more successfully by the methanol extract than by methanol/aqueous isolates, acetone, hexane, ethyl acetate, and chloroform, according to the DPPH assay's assessment of B. monnieri's hydroxyl radical scavenging properties. The methanolic excerpt of B. monnieri was also shown to have a protective action against DNA damage and a

dependent upon dosage capacity to neutralize free radicals (Aguiar *et al*., 2013). By chelating Fe, Bacopa therapy significantly decreased lipid peroxidation caused by FeSO and cumene hydroperoxide in animal models. Ethanol and B. monnieri aqueous extracts' radical-quenching action was also extensively documented (Simpson *et al*., 2015). The epithelial cell line of the lung L132 cells are exposed to sodium nitroprusside (SNP), a generator of reactive oxygen species (RNS), as a nitric oxide (NO) donor in order to assess the impacts of B. monnieri concentrate on lipid peroxidation and the generation of ROS. As a result of preventing RNS from being generated in SNP-treated cells, the prior level of nitrosative stress was dramatically reduced when B. monnieri extract was used. The prior treatment with B. monnieri extract prevented SNP-induced damage by preserving mitochondrial integrity and reducing the activity of caspase 3, cytochrome c, and Bax is enhanced in addition to the down-regulation of Bcl2 expression (Banerjee *et al*., 2021). This suggests that B. monnieri extract has a cytoprotective function. B. monnieri's methanolic extract and its separated component, bacoside A, shown significant wound-healing property. These findings imply that B. monnieri may be beneficial for treating human conditions where the generation of free radicals is a major factor. Strong antioxidant qualities that include the adsorption and neutralization of free radicals through the decomposition of peroxides or the quench of singlet oxygen are displayed by B. monnieri extracts (Brimson *et al*., 2020). Glial cells have been shown to create NO through an enzyme-independent method in response to superoxide radical stimulation. S-nitroso-N-acetyl-penicillamine (also known as SNAP) is a unique source of nitric oxide. Russo *et al*. investigated the impact of B. monnieri's extract of methanol towards SNAP-induced toxicity in rat astrocytes. According to their findings, treating with B. monnieri extract reduced the amount of reactive species and DNA fragmentation that SNAP-induced in a dose-dependent way (Russo *et al*., 2003).

Moreover, B. monnieri reduces the oxidative stress brought on by lead exposure in several rat brain regions. Exposure to lead increased the metal content, carbonyl fraction in total protein, lipid peroxidation, and ROS levels in brain tissues of rat. Pretreatment with B. monnieri shielded against lead toxicity and stopped these oxidative alterations (Simpson *et al*., 2015).

2.4.1. *Bacopa monnieri in Cancer*

Earlier reports from multiple researchers have indicated B. monnieri's antitumor potential in cancer. Human breast cancer stem cells MCF-7, Human cancer of the breast cell line and human colorectal adenocarcinoma HT-29 A-498 were tested for anticancer effects of bacoside A from B. monnieri's entire plant (Ghosh *et al*., 2021). By lowering the level of oxidation of lipids and increasing the level of antioxidants —possibly via its Action of Bacoside in Foraging Free Radicals A exhibits its chemo-preventive properties against cancer caused by diethyl nitrosamine (DEN), as demonstrated by (Janani *et al*., 1997). Rats' 3-methylcholanthrene-induced brosarcoma also revealed the antioxidant and cancer-inhibiting capabilities of B. monnieri. In addition to lowering the fatty acid peroxidation rate and downregulating cancer development indicators, B. monnieri supplementation improved the status of antioxidant enzymes (Sukumaran *et al*., 2019). Using bioassay-guided methodologies, Peng and colleagues discovered that out of the five unprocessed batches, the n-Butanol fraction of the extract made from methanol exhibited the strongest anticancer activity throughout the whole B. monnieri species and four distinct portions. In vitro cytotoxicity studies in a variety of human carcinoma stem cells, the potential anticancer activity of dammarane triterpene saponins derived from n-Butanol fraction was established by the following experiments: ninety percent and 84.13% inhibition in mice impregnated with sarcoma S180 in vivo at a dose of 50 μmol/kg, respectively. These experiments included MDA-MB-231, SHG-44, HCT-8, A-549, and PC-3M. At 50 μM, significant suppression of invasion by matrigel, movement, and adherence was seen in human breast carcinoma cell line MDA-MB-231 in vitro, according to additional research (Y. Zhang *et al*., 2022). In both untransformed (buccal) and transformed (kb oral cancer) cells, researchers investigated the protection of B. monnieri's bacoside fraction against apoptosis caused by oxidation. The results are noteworthy because they indicate that bacoside-treated buccal cells exhibit anti-apoptosis, while bacoside-treated kb oral cancer cells exhibit a sharp rise in apoptotic cells. It is evident from these studies that the toxicity generated by bacosides is specific to cancer cells and does not affect normal cells (Abdul Manap *et al*., 2019).

2.4.2. *Mechanism of Action*

Among the several pharmacological effects of *Bacopa monnieri* include protection against peptic ulcers, cardiotonic effects, anti-inflammatory, anticonvulsant, and antioxidants. In Research has demonstrated the antioxidant properties of Bacopa leaf powder. Bacopa is known to have a class

of saponins known as bacosides, which are thought to be responsible for improving cognitive function. Brahma alcoholic extract and pure bacosides A and B may improve memory, learning capacity, and cognitive function (Abdul Manap *et al.*, 2019).

Among the potential pathways that could result in improved cognition include muscarinic cholinergic receptor binding, choline acetylase activity, and modulation of acetylcholine release. The hippocampus is shielded by the saponins in Bacopa, which also regulate the output of the hypothalamic-pituitary-adrenal (HPA) gland. On activated microglial cell cultures, Bacopa has an anti-inflammatory effect. Any damage causes the microglial cells to change into a neurotoxic or neuroprotective phenotype, which releases cytokines that promote inflammation (Sukumaran *et al.*, 2019).

TNF alpha and IL-6 release from activated N9 microglial cells in vitro was found to be strongly inhibited by tea, infusion, alkaloid preparations of Bacopa, and injection of bacoside A in one investigation. Activation of choline acetyltransferase, decrease of beta-amyloid, inhibition of acetylcholinesterase, enhancement of cerebral blood flow, and monoamine potentiation are some of the mechanisms of action documented in other studies. Many aspects of Bacopa's neuroprotective properties have been researched (Valotto Neto *et al.*, 2024).

Reduction of protein carbonyl levels in cytosol and mitochondria across the whole brain has been reported as a protective mechanism of Bacopa against oxidative injury. In the prefrontal cortex, striatum, and hippocampal regions of rats, there is proof of the inhibitory action of Bacopa in preventing lipid peroxidation (Neto *et al.*, 2024). Superoxide dismutase is the first antioxidant to protect against free radicals; its levels rise in response to oxidative stress. Research revealed that after treatment, the activity of superoxide dismutase in diabetic rats was reduced to normal levels. Between the oxidant and antioxidant species, this implied equilibrium. Oxidative stress caused diabetic rats to have considerably lower glutathione levels than non-diabetic rats. The number 36 Reduction of glutathione has been observed to be enhanced by Bacopa (Simpson *et al.*, 2015).

When exposed to oxygen, almost all living things include the common antioxidant enzyme catalase. Male, middle-aged, and elderly rats' lymphocytes showed a much higher age-associated reduction in catalase activity compared to those rats treated with Bacopa. Bacopa has been demonstrated to boost the body's adaptive reactions to stress in animal tissue models. In stress-reduction experiments, it restores normal levels of cortisol and monoamine (Simpson *et al.*, 2015).

Bacopa has a generally soothing impact due to its sedative properties. Research has demonstrated that bacopa may enhance the synthesis of GABA, which lowers cell excitability and enhances the ability to make quick decisions. There is a neurotransmitter called gamma-aminobutyric acid (GABA) that quiets the brain. GABA has been demonstrated to be increased by bacopa monnieri through upregulating glutamate decarboxylase and increasing the GABA (Sadaqat *et al.*, 2023).

2.5. Nanomaterials

Nanomaterials are materials with a size of about 10^{-9} meters, on the nanometer scale. They can also be defined as materials with at least one dimension less than 100 nanometers. This small size translates to one-billionth of a meter. A unique property of nanomaterials is their ability to be manipulated at the nanoscale to control their shape and size. Nanomaterials come in various shapes depending on their dimensions, including nanosheets, nanoparticles, and nanorods (Ramesh *et al.*, 2009).

2.5.1. Classification of Nanomaterials by Dimension

Nanomaterials can be classified into four types based on their dimensionality:

2.5.1.1. Zero-Dimensional Nanomaterials (0-D)

In this type, all three dimensions are at the nanoscale. Examples include nanoparticles and quantum dots (V. Singh *et al.*, 2020).

2.5.1.2. One-Dimensional Nanomaterials (1-D)

One dimension falls within the nanoscale range, while the other two remain outside. Examples include nanowires, nanotubes, and nanorods (V. Singh *et al.*, 2020).

2.5.1.3. Two-Dimensional Nanomaterials (2-D)

Two dimensions are within the nanoscale range, and the remaining one dimension is outside. Examples include nanocoatings, nanolayers, and nanofilms (V. Singh *et al.*, 2020).

2.5.1.4. Three-Dimensional Nanomaterials (3-D)

All three dimensions are larger than the nanoscale range. These are also called bulk nanomaterials. Examples include core-shells, bundles of nanowires and nanotubes, and nanocomposites (V. Singh *et al*., 2020).

2.5.2. *Nanocomposites*

Nanocomposites are solid materials with multiple phases. In a nanocomposite, only one phase has a dimension smaller than 100 nanometers. The key difference between nanocomposites and traditional composites is their high surface area to volume ratio. Nanocomposites exhibit various physicochemical properties depending on their size and shape. Metal matrix nanocomposites (MMNCs), polymer matrix nanocomposites (PMNCs), and ceramic matrix nanocomposites (CMNCs) are some of the different types. The primary function of a nanocomposite is to interact with surrounding materials (Komarneni *et al*., 1992).

Recent developments in Graphene-Based Composites scientists are currently developing composites based on graphene. Graphene is a carbon molecule arranged in a hexagonal lattice structure. It has a zero band gap and utilizes graphene oxide (GO) as a precursor, which has low electrical conductivity. Therefore, GO is converted to reduced graphene oxide (rGO) to achieve good electrical conductivity. Graphene nanocomposites exhibit various functionalities, including cytotoxicity, photocatalysis, drug delivery, gas sensing, and photovoltaics (Papageorgiou *et al*., 2017).

2.5.3. *Nanomaterial Synthesis Methods*

Nanomaterials can be synthesized using three main methods:

1. Biological method
2. Chemical method
3. Physical method

2.5.3.1. Biological Method

The biological method is a single-step, eco-friendly, and simple approach. It utilizes various plant parts and microorganisms to produce nanomaterials (Ingale *et al*., 2013).

2.5.3.1.1. Using Microorganisms

Bacteria, algae, and fungi can be used to create nanomaterials from aqueous solutions of metal salts (Jadoun *et al*., 2022).

2.5.3.1.2. Using Bacteria

This method leverages proteins and other minerals from living organisms to prepare nanomaterials through a process called bio-mineralization. For instance, magnetotactic bacteria found in deep-sea anaerobic environments produce magnetosomes, protein-coated structures containing nano-sized magnetic iron crystal oxide, to create their habitat. In medical applications, magnetosomes are used for hyperthermia due to their good magnetic conductivity (Iravani *et al*., 2011). Photosynthetic bacteria can generate nanoparticles sized 10-20 nanometers using NADH (nicotinamide adenine dinucleotide) and dependent reductase, which play a significant role in reducing gold ions to produce gold nanoparticles. Pseudomonas cells are also employed to synthesize palladium nanomaterials and nanoparticles. Studies have shown that the pH level in the growth medium can influence the shape and morphology of the nanoparticles. *Rhodopseudomonas capsulata* has been demonstrated to produce gold nanoparticles of varying sizes, with the shape regulated by the pH. Bacteria are considered potential biofactories for producing various nanoparticles, including those of selenium, silver, palladium, gold, platinum, titanium, magnetite, titanium dioxide, cadmium sulfide, and other metals (Pantidos *et al*., 2014).

2.5.3.1.3. Using Fungi

Fungi like Fusarium oxysporum can be used to produce silver nanomaterials and nanoparticles. Nanomaterials and nanoparticles prepared using fungi are known for their high stability and abundant protein secretion. These materials find applications in various industries, including paper, textiles, food, and medicine (A. U. Khan *et al*., 2018).

2.5.3.1.4. Using Algae

Algae called *Sargassum wightii* can be used to synthesize extracellular gold nanomaterials and particles. This method achieves a 95% production yield within a 12-hour incubation period. However, research on algae for nanomaterial and nanoparticle synthesis is still limited (Castro *et al*., 2013).

2.5.3.2. Chemical Method

The chemical method involves using chemical reactions to produce nanomaterials. This method offers good control over the size and shape of the nanoparticles. However, it can also generate hazardous chemicals as byproducts (Talapin *et al*., 2016).

The chemical pathway consists of many techniques such as thermal breakdown, sonochemical, coprecipitation, microemulsion, hydrothermal, and electrochemical deposition. Microemulsions, sol-gel syntheses, sonochemical reactions, hydrothermal reactions, hydrolysis and thermolysis of precursors, flow injection syntheses, and electrospray synthesizes are just a couple of the chemical techniques used to produce magnetic nanoparticles for use in medical imaging. Chemical vapour deposition techniques are useful in the creation of nanoparticles based on carbon. Vapor deposition of chemicals finds an ideal precursor to have the following characteristics: low cost, long shelf life, high chemical utmost purity prolonged evaporation strength, and acceptable volatility. Additionally, no pollutants should remain after its breakdown (Panigrahi *et al*., 2004). Multilayered graphene is produced using chemical vapor deposition when Ni and Co catalysts are used, while monolayer graphene is produced with a Cu catalyst. Two-dimensional nanoparticles are commonly produced via chemical vapor deposition is a useful method for producing high-quality nanomaterials (Y. Zhang *et al*., 2013). For the development of nanomaterials, a wet chemical technique called sol-gel is frequently used. Numerous excellent metaloxide-based nanomaterials are produced using this method. The sol-gel process offers several benefits, such as low processing temperature, uniform material generation, and a straightforward method for creating complex nanostructures and composites. Finally, the process is economical. It is shown by the microscopic and monodispersed nature of the NPs produced that how to make magnetic lipase-immobilized NPs using the reverse micelle approach. You can modify the size of the carbon chain in surfactant materials or add more substances that enlarge pores to change the pore

diameters of nanoporous materials. Some examples of materials containing nanostructured that can be created using the soft template approach are mesoporous polymers, carbonaceous nanospheres, porous aluminas, single-crystal nanorods, and mesoporous N-doped graphene (Ciriminna *et al*., 2013). Recent advances in engineering nanomaterials have focused a lot of attention on the hydrothermal approach assisted by microwaves, which combines the benefits of hydrothermal and microwave processes. Various nanogeometries of materials, including nanorods, nanowires, nanosheets, and nanospheres, can be created in an intriguing and useful way using hydrothermal and solvothermal techniques (Chae *et al*., 2017).

2.5.3.3. Physical Method

Many techniques are included in the physical route or mechanism, such as powder milling with balls, gas-phase depositions, electron beam lithographic processes, and ablation by pulsed laser, spray, and laser-induced pyrolysis and laser-induced pyrolysis. By impacting the material of interest with a strong laser beam, development by laser ablation produces nanomaterials. The intense laser radiation causes, the initial content, or forerunner to vaporize during the ablation using laser procedure, creating nanoparticles (Harish *et al*., 2023). Many kinds of nanomaterials, include metallic nanoparticles, oxide composites, carbon nanomaterials, and ceramics, can be manufactured using this technique. Lithography is an important method for building nanoarchitectures; it makes use of an intense light or electron beam. Lithography comes in two main varieties: maskless and mask-less. Masked nano-lithography transfers patterns of nanomaterials over an extensive surface region by employing a preset mask or blueprint. Photo-lithography, soft lithography, and nano-imprint lithographic process are a few masked lithography approaches. Making nanoscale items from bigger particles can be done inexpensively via mechanical milling. In order to combine different phases efficiently and to create nanocomposites, mechanical milling is a beneficial technique (Tahir *et al*., 2021). Energy storage, energy conversion, and environmental remediation are among the applications for ball-milled carbon nanoparticles. The electrospinning method is among the simplest ways to create nanostructured materials. Many materials, most notably polymers, can be used to create nanofibers using this technique. This approach has led to the development of organic, inorganic, porous polymer, and core-shell composites. By saturating the intended surface equipped with strong ions in state of gas, sputtering deposition produces the tangible ejection of small groups of atom. The utilization of

sputtering is attractive because it is less costly than electron-beam lithography and produces nanomaterials with an arrangement that is closer to the desired material and less contaminated (Fahrner *et al*., 2005).

2.5.3.4.   Techniques for Nanoparticles Synthesis

This technique uses two strategies. 1) A top-down strategy, and 2) A bottom-up strategy. The nanomaterials in the top-up approach are created using mechanical methods. Larger particles are divided into smaller ones in these. The primary disadvantage of the top-up strategy is that nanomaterials and nanoparticles cannot be produced in the appropriate size and shape. On the other hand, a chemical combination of smaller ions is used in the bottom-up technique. It is either liquid or gaseous. Both the condensation process and the utilization of smaller particles to create larger particles take place in this (Talapin *et al*., 2016).

2.5.3.4.1.   Top-down approaches

Nanostructured materials are created by dividing bulk materials using top-down methods. Top-down methods include mechanical sputtering, etching, milling, laser ablation, and electro-explosion (Hutchinson *et al*., 2000).

2.5.3.4.1.1.   Mechanical milling

When working with bulk materials, mechanical milling is an affordable way to create substances on a nanoscale. The production of phase blends and mechanical milling can help with both the development of nanocomposites. Depicts the basic idea behind the ball milling technique. Copper, nickel, magnesium, and oxide- and carbide-based nanoalloys, wear-resistant spray coatings, and a range of additional materials for nanocomposite are all made by mechanical milling, Energy conversion, energy storage, and environmental cleanup requirements can be met by using carbon nanoparticles produced by ball milling, which are regarded as a unique class of nanomaterial (D. J. P. i. M. S. Zhang *et al*., 2004).

2.5.3.4.1.2.   Electrospinning

Of all the top-down techniques for creating nanostructured materials, electrospinning is one of the easiest. Many other materials can be used to create nanofibers, although polymers are the most prevalent choice, A notable development in electrospinning technology was coaxial

electrospinning. There are two coaxial capillaries in the spinneret in coaxial electrospinning. To achieve ultrathin fibers of core-shell on a broad scope, coaxial electrospinning is a straightforward and efficient top-down method. One can enlarge these incredibly thin nanomaterials to several centimeters in length. This method has produced inorganic, organic, and hybrid compounds as well as core-shell and hollow polymeric materials (Bhardwaj *et al*., 2010).

2.5.3.4.1.3. Lithography

Using an electron or light beam that is focused, lithography is a helpful technique for creating nanostructures. Mask-free and mask-covered lithography are the two primary subtypes of this process. A unique cover or emulate is used in masked nanolithography. To distribute nanopatterns over an extensive surface area. Soft, photo, and nanoimprint lithography are examples of masked lithography. Focused ion beam lithography (FIB lithography), electron beam lithography, and scanning probe lithography are all kinds of maskless lithography. Arbitrarily writing nanopatterns without the use of a cover is possible with maskless lithography (Thompson *et al*., 1983).

2.5.3.4.1.4. Sputtering

Using a technique called sputtering, high-energy particles like gas or plasma are blasted onto solid surfaces to form nanomaterials. For creating thin films of nanomaterials, sputtering is thought to be a useful technique. A method known as the target surface comes into contact with powerful gaseous ions during sputtering deposition, which, depending on the energy of the impacting gaseous ions, physically expel tiny atom clusters. Many techniques, including magnetron, radio-frequency diode, and DC diode sputtering, can be used to carry out the sputtering procedure. The sputtering gas is usually supplied to an evacuated chamber, where sputtering is generally carried out. Free electrons crash into the gas in the cathode target when a high voltage is applied, creating gas ions. Atoms are ejected off the cathode target's surface as a result of the positively charged ions' tremendous acceleration toward it in the electric field and constant collision. When considering cost-effectiveness in comparison to electron-beam lithography, the sputtering process is appealing since the composition of the sputtered nanomaterial stays the same as the target material with fewer imperfections (Sigmund *et al*., 1969).

Using a technique called sputtering, high-energy particles, such as plasma or gas are blasted onto solid surfaces to form nanomaterials. For creating thin films of nanomaterials, sputtering is considered to be a useful method. A method known as the target surface comes into contact with powerful gaseous ions during sputtering deposition, which, depending on the striking gaseous ions' energy, physically expel tiny atom clusters many techniques, including magnetron, DC diode sputtering, and, radio-frequency diode can be used to carry out the sputtering procedure. Sputtering is typically done in an empty chamber that receives the sputtering gas. Free electrons crash into the gas in the cathode target when a high voltage is applied, creating gaseous ions. The positively charged ions accelerate tremendously toward the cathode target in the electric field, ejecting atoms from its surface and constant collision. When considering cost-effectiveness in comparison to electron-beam lithography, the chemistry of the sputtered nanomaterial remains the same as the target material with fewer defects, which makes the sputtering technique attractive (Kelly *et al*., 2000).

2.5.3.4.1.5.   The arc discharge method

Different types of nanostructured materials can be produced with the help of the arc discharge process. Production of carbon-based materials, including carbon nanohorns (CNHs), few-layer graphene (FLG), fullerenes, carbon nanotubes, and amorphous spherical carbon nanoparticles, is its predominant characteristic. When it comes to producing fullerene nanomaterials, the arc discharge approach is quite significant. Within a container that sustains a particular helium pressure, the forming process modifies two graphite rods. Since fullerene cannot be synthesized in the presence of moisture or oxygen, it is crucial to occupy the chamber entirely with helium. The arc discharge that occurs causes the carbon rods to vaporize is the space between the graphene rods' ends (Ando *et al*., 2006).

In order to create novel types of nanomaterials, arc discharge circumstances are crucial. Explains the parameters under which the arc discharge process forms various carbon-based nanomaterials. Since the method of arc discharge collects different nanomaterials based on carbon at varied points because of their differing development methods. MWCNTs, pyrolytic graphene, high-purity polyhedral graphene particles, and nano-graphite particles could be extracted from arrays at both electrodes from the anode or cathode. Nanomaterials with a carbon basis can be extracted from the inner chamber additionally to the electrodes. Numerous morphologies of single-wall carbon nanohorns (SWCNHs) can be created from various atmospheres. To illustrate, while "dahlia-like"

SWCNHs are created under ambient circumstances, "bud-like" SWCNHs are generated in CO and CO2 atmospheres. One effective way to produce graphene nanostructures is by the arc discharge method. Properties of graphene can be influenced by the conditions that exist during synthesis (Subrahmanyam *et al*., 2009).

2.5.3.4.2.   Bottom-up approaches

2.5.3.4.2.1.   Chemical vapor deposition (CVD)

Chemical vapor deposition methods are used to produce carbon-based nanomaterials are very important. Precursors in the vapor phase react chemically to generate a thin sheet on the substrate surface in CVD. A forerunner is deemed appropriate for CVD if it possesses the following qualities: low cost, non-hazardous nature, good stability during evaporation, high chemical purity, and extended shelf life (Creighton *et al*., 2001). Additionally, no leftover contaminants should emerge from its breakdown. When carbon nanotubes are produced via CVD, for example, an oven is used for heating a substrate to very high temperatures. The next step is to gradually add a precursor gas that contains carbon, like hydrocarbons, to the system. When gaseous matter decomposes at elevated temperatures, carbon atoms are released and combine again to produce carbon nanotubes on media. The nature and form of the resulting nanomaterial, however, are greatly influenced by the catalyst of choice. Monolayer graphene is produced by a Cu catalyst in the CVD-based graphene production process, while multilayer graphene is produced by Ni and Co catalysts. One crucial method for producing two-dimensional nanoparticles is CVD (Rashid *et al*., 2015).

2.5.3.4.2.2.   Solvothermal and hydrothermal approaches

The hydrothermal process is one of the most extensively used and well-liked methods for producing nanostructured materials. The hydrothermal approach produces nanostructured materials via a heterogeneous reaction in a solution of water at high pressure and temperature close to the critical point inside a sealed vessel. Solvothermal and hydrothermal methods are same to each other. The sole difference is that it's carried out in a non-aqueous medium. Solvothermal and hydrothermal processes are usually carried out in closed systems. In the area of nanomaterials engineering, the microwave-assisted hydrothermal approach has been receiving a lot of attention recently since it integrates the best features of both hydrothermal and microwave techniques. Using intriguing and useful methods like solvothermal and hydrothermal processes, one can create

various nano-geometries of materials, such as nanowires, nanorods, nanosheets, and nanospheres (Gan *et al*., 2020).

2.5.3.4.2.3.   The sol–gel method

A common wet-chemical technique for producing nanoparticles is the sol-gel method. High-quality metal-oxide-based nanomaterials of various kinds have been produced using this technique. This approach is known as the "sol-gel method" because, this process of creating the metal-oxide nanoparticles, the prelude liquid transforms into a sol, which is then transformed again form a gel, a type of interconnected structure following condensation, the solvent's viscosity rises to create pores containing structures that are then allowed to mature (Hench *et al*., 1990). During the course of the condensation or poly-condensation process, oxy- (M–O–M) or hydroxo- (M–OH–M) connections form, resulting in the formation of metal–hydroxo– or metal–oxo–polymers in solution. There are alterations to the properties, features, and porosity of polycondensation as it proceeds with age. A decrease in porosity and an increase in the spacing between colloidal particles occur with age. Aqua and organic solvents are eliminated out of the gel during the drying phase that follows the aging phase. In order to produce nanoparticles, calcination is the final step. Demonstrates how films and powdered substances are made by the sol-gel method. Many variables, including a kind of forerunner, hydrolysis rate, ageing duration, molar ratio and pH of the precursor to H2O, influence the end product that is manufactured using the sol–gel process.75% Besides being a low processing temperature, the created material is homogenous, and the sol-gel technique is an easy way to create complex nanostructures and composites. It is also a cost-effective technique (Bokov *et al*., 2021).

2.5.3.4.2.4.   Methods of soft and hard templating

Compounds with nanoporous structure can be produced by a variety of soft and hard template processes. For the creation of nanostructured materials, a straightforward conventional technique is the soft template methodology. Because it is easy to use, has relatively gentle experimental conditions, and produces diverse morphologies of components, the soft template method has been seen as beneficial. Using a variety of the soft templating mode is used to produce nanoporous compounds from soft templates, such as anionic, cationic, and non-ionic surfactants, elastic organic molecules, and block copolymers (Yang *et al*., 2015). Electrostatic, van der Waals, and hydrogen bonding forces are the main ways in which precursors and soft prototypes engage in interaction. Soft prototypes are used to create 3D organized mesoporous structures containing

precisely liquid crystalline micelles with a framework are utilized. The synthesis of mesoporous materials employing alkyl trimethyl ammonium surfactant, for example, hexagon-shaped (MCM-41) laminated (MCM-50), square (MCM-48), and ordered mesoporous silicas, is one of the primary examples. In general, the soft templating approach uses two processes to produce structured mesoporous materials: collaborative self-assembly and "true" liquid-crystal templating (Petkovich *et al.*, 2013). Many parameters, including concentrations of surfactant and precursor, the chemical structure of the surfactant being used the ratio of surfactant to counterpart, and external variables can affect the mesoporous material configurations produced by 3D ordered micelles. To modify the pore widths of nanoporous substances, one can alter the carbon chain-length of the surfactant substances or add more pore-expanding compounds. By using a soft template, it is possible to produce a wide range of nanostructured compounds, such as mesoporous polymeric carbonaceous nanospheres (Bruckner *et al.*, 2021).

One other term for the rigid template method is nano-casting. Precursor molecules are introduced into the solid template pores, which are then filled to create the desired nanostructures for the intended uses an organized mesoporous material can only be created by carefully choosing the hard template. Ideally, these inflexible templates should be simple to separate without compromising the resulting nanostructure and maintain a mesoporous structure during the preliminary conversion procedure (Lu *et al.*, 2006).

Among the materials are wooden shells, colloidal crystals, particulates, carbon nanotubes, silicon dioxide, and carbon black that have been employed as hard templates. To obtain nanostructures by templating methods, there are three basic phases in the synthetic pathway. First, the suitable original template is created or chosen. After that, a specific precursor is added in order to transform the template mesopores into an inorganic solid. Finally, to obtain the mesoporous duplicate, the original template is eliminated. Mesoporous templates can be used to manufacture various nanoparticles such as nanorods, nanowires, 3D nanostructured materials, and nanostructured metal oxides (Wohlleben *et al.*, 2017).

2.5.3.4.2.5.   Reverse micelle methods

The reverse micelle technique can also be utilized to create nanomaterials with appropriate dimensions and geometries. Conventional micelles are generated in an oil-in-water emulsion; their hydrophobic tails point in the direction of a core that is confined by oil droplets. Conversely, reverse micelles develop in a water-in-oil emulsion when the hydrophilic heads are oriented toward

a water-containing core. The reverse micelle's primary role is that of an apparatus for creating nanoparticles using a nanoreactor (Correa *et al.*, 2012). It serves as a storage facility for nanomaterials' progress. The diameters of these nanoreactors can be varied, which will alter the size of the nanoparticles produced by this method by varying the water-to-surfactant ratio. Smaller water droplets mean smaller nanoparticles will form if the concentration of water is reduced. Hence, a simple approach to producing consistent nanoparticles with carefully regulated sizes is offered by the reverse micelle method. Remarkably little and uniformly distributed in nature are the nanoparticles produced by the reverse micelle technique, demonstrates the construction of magnetic lipase-immobilized nanoparticles using the reverse micelle approach (Sun *et al.*, 2019).

CHAPTER 3: MATERIAL AND METHOD

3.1. Materials:

Weight Balance, Burette, Magnetic Stirrer, Centrifuge Machine, Microwave Oven, Thermometer, Autoclave, Culture Plates, Conical Flask, Quartz Cuvettes, Test tubes, Funnel, Refrigerator, Whatman's Filter Paper, Beaker, pH Meter, Pipettes, Tips, Measuring Flask, Grinder, Incubator, Glass Rod, Measuring Cylinder, Falcon Tubes, Cell Scrapers, Laminar Flow, Pestle Mortar, 96-well plates, Cell Culture Incubator (at 37°C in 5% CO_2), T25 flasks.

3.2. Chemicals:

Sorafenib (Nevexar) drug, Copper chloride salt, Calcium chloride salt, Zinc chloride salt, Ethanol (99% & 70%), Distilled water, MCF-7 cell lines, Phosphate Buffered Saline (PBS), Dulbecco's Modified Eagle Media (DMEM), 10% Fetal Bovine Serum (FBS), 1% penicillin-streptomycin, 1X trypsin-EDTA.

3.3. Preparation of plant leafs extract

3.3.1. Collection of Plant

Bacopa monnieri leaves were used in the present study, which were collected from the Bank of Namal Lake, Mianwali, Pakistan.

Figure 3.1: Collection of Plant Leaves

3.3.2. Washing of leaves

After collection of bacopa monnieri fresh leaves were thoroughly washed with tap water and then with Distilled water. After washing, to remove the impurities the ethanol is sprays on the leaves.

Figure 3.2: Washing of Leaves

3.3.3. Drying of Leaves

After washing, the leaves dried in shade for almost 3 weeks.

Figure 3.3: Drying of Leaves

3.3.4. Grinding of leaves

After completely drying of leaves, leaves were grind in grinder first and then converted into fine powder by pestle and mortar.

Figure 3.4: Grinding of Leaves

3.3.5. Plant Extract Synthesis

20g of Bacopa Monnieri leaves powder was measured on measuring balance. After measuring, mixed leaves Powder in 200ml of distilled water in conical flask. Now put solution of Bacopa monnieri on magnetic stirrer and boil at 60°C while continuing stirring for 2 hours. After 2 hours, the green color of plant solution was changed into pale green color which indicates plant extract formation.
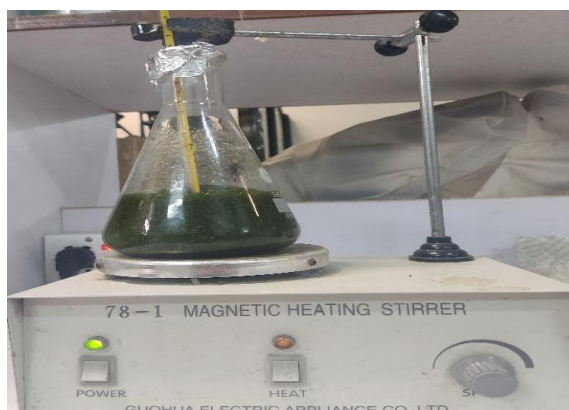
Figure 3.5: Preparation of Plant Extract

3.3.6. Centrifugation of Extract

After preparation of plant extract, extract was put in falcon tubes and centrifuged for 15 minutes at 3000-4000 rotation per minutes (rpm). The supernatant was collected and the pallets residing in falcon tubes were discarded.
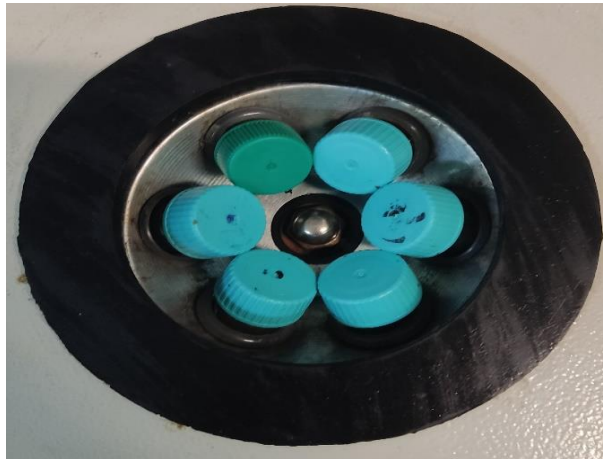
Figure 3.6: Centrifugation of Extract

3.3.7. Filtration of extract

After centrifugation, filtered the extract with Whatman's filter paper no.1 in conical flask.

Figure 3.7: Filtration of Extract

3.3.8. Extract pH maintenance

After Filtration, maintained pH of extract with pH meter. The initial pH of extract was 6.5 then it changed into 9 by adding 0.5M of NaOH with the help of dropper.

Figure 3.8: Extract pH maintenance

3.4. Preparation of Nanoparticles

3.4.1. Copper Formulated Nano-Coated Drug Formation

The filtrate leave extract was taken for further experimental use. 15 ml Copper chloride (1.5g copper chloride salt + 15ml distilled water) was taken in conical flask and 10ml of Sorafenib drug (0.9g of Sorafenib drug + 10ml water) was added in the flask containing copper chloride solution, and then through titration method 25 ml of bacopa monnieri leaf extract was added through burette, while solution kept on constant stirring. This was kept in magnetic stirrer for 1.5 hours in 80ºC. After this, the mixture was coated with calcium chloride by adding 25 ml calcium chloride (2.5g calcium chloride + 25ml distilled water) into flask and then 25ml bacopa monnieri leaf extract was added through titration while keeping on constant stirring. Then the solution is kept overnight in room temperature.

3.4.2. Zinc Formulated Nano-Coated Drug Formation

The filtrate leave extract was taken for further experimental use. 15 ml Zinc chloride (1.5g Zinc chloride salt + 15ml distilled water) was taken in conical flask and 10ml of Sorafenib drug (0.9g of Sorafenib drug + 10ml water) was added in the flask containing copper chloride solution, and

then through titration method 25 ml of bacopa monnieri leaf extract was added through burette, while solution kept on constant stirring. This was kept in magnetic stirrer for 3 hours in 60ºC. After this, the mixture was coated with calcium chloride by adding 25 ml calcium chloride (2.5g calcium chloride + 25ml distilled water) into flask and then 25ml bacopa monnieri leaf extract was added through titration. Then the solution is kept for 2 hours at 65ºC.
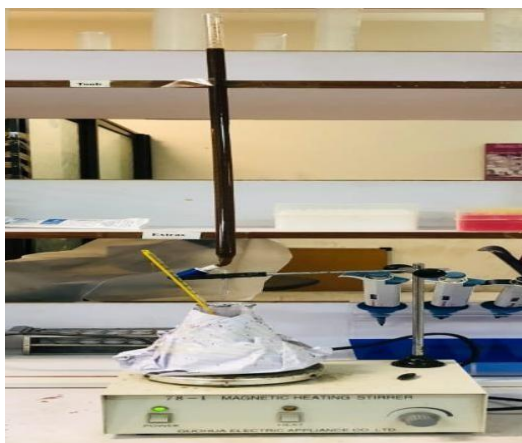
Figure 3.9: Titration Process

3.4.3. *Centrifugation*

The mixture was put in falcon tubes and centrifuged for 15 minutes at 3000-4000 rotation per minutes (rpm). Supernatant was discarded and pallet is kept.

Figure 3.10: Centrifugation

3.4.4. Washing

After that the pallet was washed three time using distilled water to remove inorganic debris.

Figure 3.11: Nanoparticle Washing

3.4.5. Drying

After washing, the solution is poured in a wide Petri dish and placed in oven at 70℃ for overnight so it would dry fully.
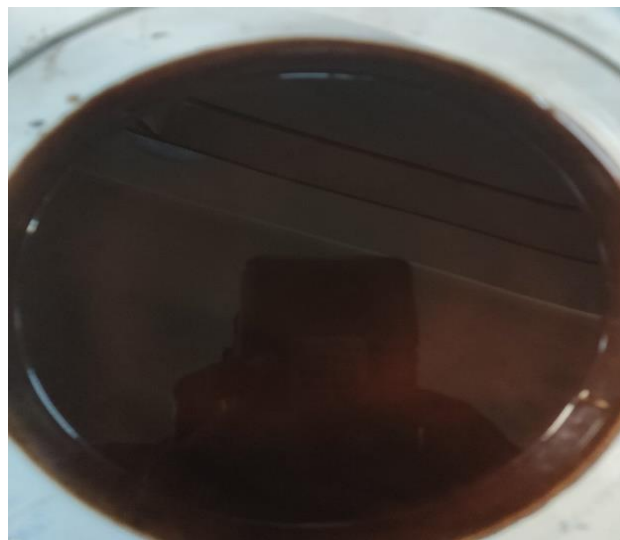
Figure 3.12: Nanoparticles Plated For Drying

3.4.6. Scratching of Nanoparticles

After drying, using spatula the dried formed of nanoparticles was scratched and moved to mortar & pestle.

Figure 3.13: Scratching of Nanoparticles

3.4.7. Grinding of Nanoparticles

Using mortar pestle, nanoparticles were grinded into powder form, and moved to eppendorf tube for storage.
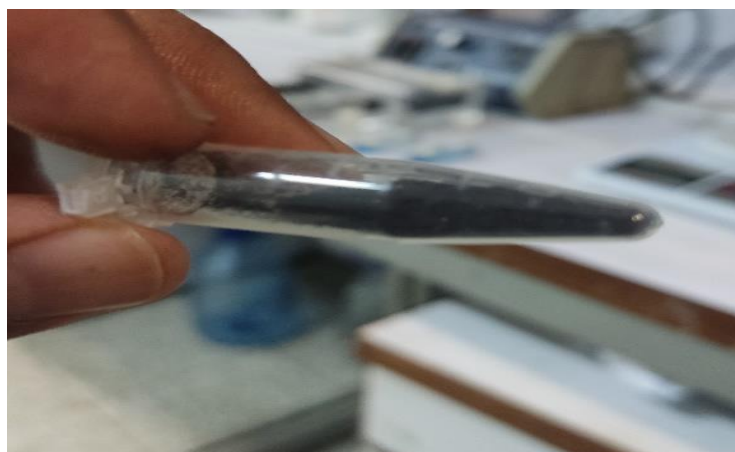
Figure 3.14: Storage of Nanoparticles in Eppendorf

3.5. Characterization of Nano-coated Drug

3.5.1. Ultraviolet - Visible (UV) Analysis

Analysis method depends on the principle that sample near the ultraviolet, visible, and infrared regions absorbs monochromatic light. According to Beer-Lambert's absorbance law, the solution's absorbance is proportional to the path length and absorbing species concentration.

UV analysis of nano-coated drugs was done to check the drug loading using UV-Spectrophotometry and absorption of drug. Spectra was recorded from range of 200nm to 700nm. Using quartz cuvettes, all spectra were obtained in solution phase.

3.5.2. Fourier Transform Infrared Spectroscopy (FTIR)

By identifying changes in functional groups in biomolecules, the Fourier transform infrared (FTIR) method of spectroscopy can be used to identify variations throughout the complete composition of microorganisms. In essence, it detects how molecules affected by infrared radiation at a certain wavelength vibrate and rotate. A beam splitter, a fixed mirror, and a moving mirror make up an interferometer that collects the IR radiation that is released by an IR source. The interference patterns used by the interferometer to measure the wavelength of emitted light serve to improve accuracy. Once IR radiation has been applied to a sample, the strength of the radiation passing through at a particular wavenumber is measured to produce an IR spectrum. Depending on the quality standards needed for the sample analysis, the number of scans can be changed. At a particular wavenumber, it is possible to detect the IR radiation of specific chemical groups. Wavenumber is represented by the x-axis of the spectrum, while absorbance or transmittance is shown by the y-axis.

Although a solid, liquid, or gas sample can be utilized for FTIR analysis, only a liquid sample was employed in this case. Diamond glasses or selected compatible IR transparent windows such as zinc selenide may be more suitable for liquid samples. Both times, as was previously mentioned, the IR beam goes through the sample. The transmittance approach is favorable because of the samples' low noise-to-signal ratio. This approach has some drawbacks, such as the time needed

for sample preparation and the fact that the absorption sensitivity changes within a sample with varying thicknesses.

3.5.3. Scanning Electron Microscopy

SEM was used to evaluate the morphological characteristics and measurements of the samples. Before examining the specimens, a thin layer of gold was sprayed on them using an ion sputter coater with a low dissolution rate. At different magnifications, photographs of the different morphologies and measurements of the specimens were captured.

3.5.4. Zeta Analysis

Zeta potential, also termed as electro-kinetic potential, is the measure of electrostatic potential on nanoparticles' surface at electrical double layer in a solution. It can provide valuable information regarding the properties, behavior, and toxicity of nanoparticles in the environmental and biological systems. Nanoparticles having the zeta potential between -10 and +10 mV are thought to be neutral while particles having the potential greater than +30 mV or less than -30 mV are strongly cationic and strongly anionic respectively. Zeta cells are used to measure the zeta potential. The sample's low ionic strength, its pH, and its concentration were measured before and after the analysis.

After loading the sample on 1 mL syringe it is transferred into the zeta cells dropwise. The zeta cells were loaded into the instrument keeping in view the temperature and voltage. Particle stability is measured by the magnitude of the zeta potential. The higher magnitude causes increased electrostatic repulsion and ultimately enhanced particle stability.

In this study, the zeta potential of nano-coated drug was checked. And the estimated range on which sample can set to be stable was from -50 mV to +50mV.

3.5.5. Dynamic Light Scattering

Also known as quasi-elastic light scattering or photon correlation spectroscopy. It is used to measure the particles size distribution in suspension. The analysis is done was the when the light scattered from a laser and passes through the sample. It provides the information about the aggregation and stability of sample and also about the particle size distribution.

In this testing, Stokes-Einstein equation is used to calculate the size of sample. When a laser beam passes through the sample in suspension form, particles scatter the light. The intensity of scattered light fluctuates over time, these fluctuations are analyzed to determine the particle's diffusion coefficient. These coefficients are used to calculate the size of particles.

3.5.6. X-Ray Diffraction

X-ray diffraction patterns of the nano-coated drug was measured using an X-ray diffractometer. At room temperature, the specimens are examined over such a diffraction angle range of $2\theta = 10°–80°$ at a scanning speed of $0.4°/min$.

3.6. Cancer cell lines

MCF-7 cell line was obtained from Professor Dr. Aneela (Atta-Ur-Rahman School of Applied Bio-Sciences (ASAB), National University of Science and Technology, Islamabad, Pakistan). Cells were cultured as adherent monolayers in tissue-treated T25 flasks in Dulbecco's Modified Eagle's media (DMEM) supplemented with 10% FBS and 1% penicillin-streptomycin from Thermo Fisher Scientific (Fair Lawn, NJ). The cells were grown in a sterile cell culture incubator at 37°C in 5% CO_2. Depending on the medium's pH, the medium was replaced two to three times a week, and cells were allowed to develop to 70% to 90% confluency.

3.6.1. Preparation of MCF-7 cell lines

When MCF-7 cells cultured in a T25 flask reached 70-90% confluency, the process of passaging was initiated. The cells were trypsinized with 1X trypsin-EDTA and incubated for 5 min at 37C to detach them from the flask's surface. Cells were then neutralized with complete growth media to stop trypsin action and provide a nutrition-rich environment. After neutralization, the cell suspension was collected into a 1.5ml centrifuge tube and centrifuged for around 5 minutes at a moderate speed to collect the detached cells into a pellet. After that, they were resuspended in a 1 ml media for counting. Cell counting was done to precisely calculate the cell density, ensuring correct seeding into a new culture flask at the required density.

3.6.2. Cell Counting

Trypan blue is a common stain used for cell counting and cell viability. Cell counting with trypan blue staining is based on the dye's differential exclusion by viable and non-viable cells. Viable cells have intact cell walls that exclude trypan blue, keeping them unstained and transparent under a microscope. In contrast, non-viable cells with ruptured or weakened membranes allow trypan blue to permeate and dye them blue. The assay was carried out by loading a hemocytometer with 10ul of cells from cell suspension mixed with 10ul Trypan blue solution. A loaded hemocytometer was placed on an inverted light microscope. Viable (unstained) and non-viable (stained) cells were counted within counting grids under a microscope to determine overall cell density and viability. After that, the average cell count, and dilution factor were calculated to determine the cell concentration.

3.6.3. Drug Treatment

3-Experimental groups were made on cell plating day. Drug group was made with dilution 15ml of (50ug of Drug/1ml PBS). Copper Formulated and Zinc Formulated nano-coated drug dilution of 15ml was made of containing (100ug samples/1ml PBS). In each well around 100ug of the samples were added and incubated for 72 hours for 37℃.

3.6.4. Transfection

The day before transfection, cells were seeded into four separate T25 flasks at a density of 0.7 x 106 cells: one for the control group and three for the experimental group (one drug group, second copper group & third zinc group). Before transfection, the plated cells were allowed to grow until they were 70-90% confluent. Cells were then incubated with the transfection mixture for six hours at 37°C and 5% CO_2 in a cell culture incubator. After incubation, the transfection mixture was gently aspirated and replaced with fresh, pre-warmed complete cell culture media containing penicillin-streptomycin. Penicillin-streptomycin was used as a selection marker to confirm the success of transfection. The next day, both the control were given concentration of 10 ug/uL and three experimental groups were given concentration of 5&10 ug/uL (Drug group 5ug/ul, copper & zinc groups were given 10ug/ul). The cells were then cultured for 48 hours in an incubator set at 37°C with 5% CO2. During the incubation time, the cells were carefully monitored to examine the

survival and proliferation of transfected cells in contrast to untransfected control cells, which served as a sign of successful transfection.

CHAPTER 4: RESULTS

4.1. Characterization of Nano-coated Drug

4.1.1. Ultraviolet-Visible Spectrometry:

The two samples of nano-coated drug were synthesized using green method and were characterized using UV-visible spectrometer, results are shown in the figure given below. From the literature, we checked that the drug absorbance is shown as 260-270nm. From the given below results we can checked and characterized that the drug was absorbed by both the samples. In copper formulated nano-coated drug the maximum absorbance peak was shown on 262nm and in zinc formulated the maximum absorbance peak was shown at 263nm. The Ca-O bond shows that peaks at 210-250nm, Cu-O shows peaks at 280-350nm, and Zn-O shows peaks at 300-350nm. The phytochemical properties reduce the catalysts quickly, leading to the increasing nano-coated drug formation, moreover enhancing the absorption values.
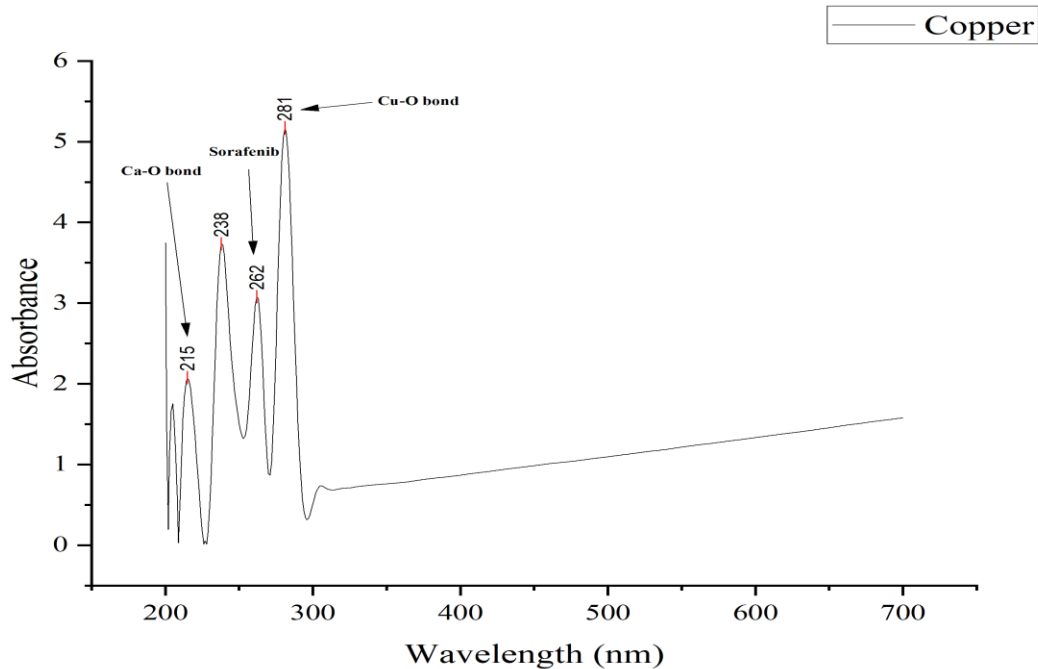
Figure 4.1: UV-Spectrophotometry Graph of Copper Formulated Nano-coated Drug
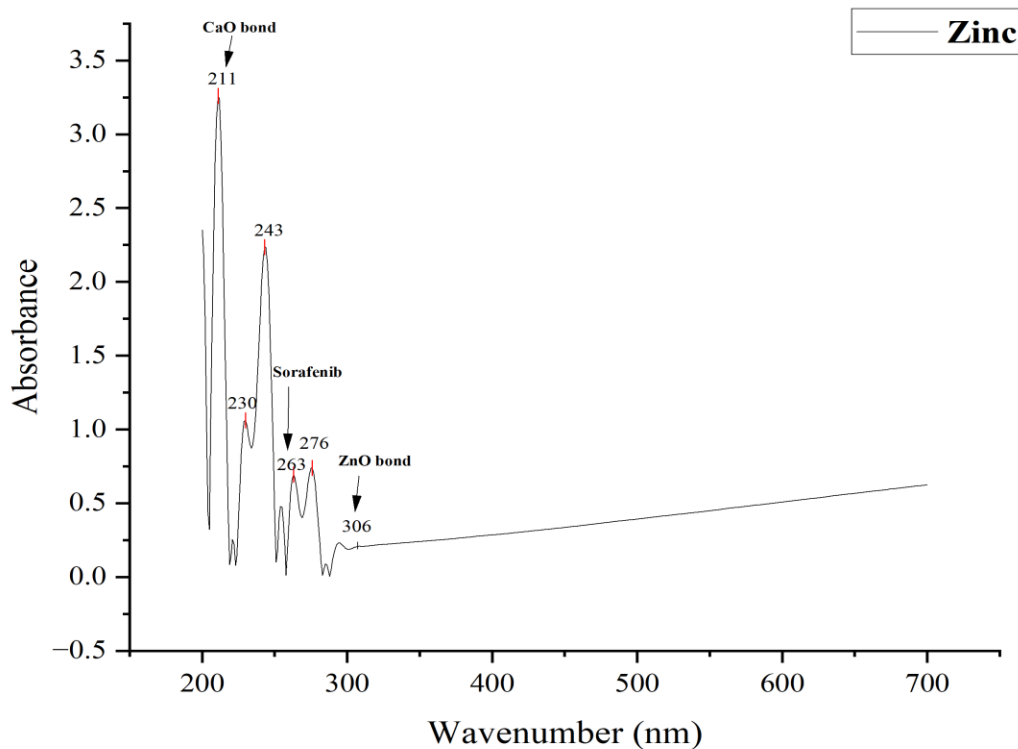
Figure 4.2: UV-Spectrophotometry Graph of Zinc Formulated Nano-coated Drug

4.1.2. X-Ray Diffraction (XRD) Analysis

XRD technique has been adopted for determining crystalline structure and phase purity of green nano-composite. The data, according to X-ray diffraction technique, is most likely crystalline nature of the composite indicating the production of nano-coated drug. The XRD spectrum of copper formulated nano-coated drug comprises of multiple diffraction peaks that were designated at 2θ angle 7.72, 12.59, 14.55, 15.85, 19.81 of sorafenib drug, 24.41, 31.41 of calcium oxide (CaO) and 67.36 of copper oxide (CuO). The diffraction patterns classified as cubic, hexagonal and monoclinic crystal system. The computed lattice constant for CuO is a= 4.6530 Å b= 3.4100 Å c= 5.1080 Å which match with the published value (JCPDS File No. 96-101-1149), and for CaO is a= 3.25 Å b= 5.20 Å which match with the published value (JCPDS File No.036-1451).
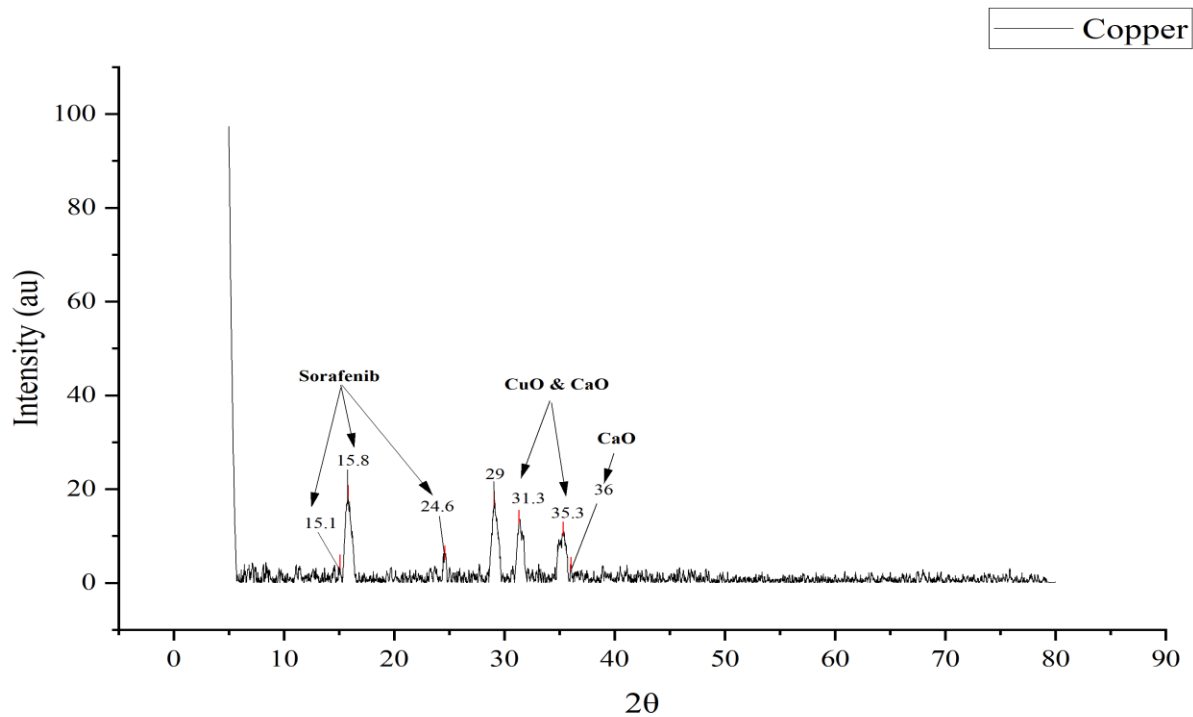
Figure 4.3: X-Ray Diffraction Graph of Copper Formulated Nano-coated Drug

The XRD spectrum of zinc formulated nano-coated drug comprises of multiple diffraction peaks that were designated at 2θ angle 12.26, 14.18 of sorafenib drug, 24.53, 31.41 of calcium oxide (CaO) and 29.10 of zinc oxide (ZnO). The diffraction patterns classified as cubic, hexagonal and monoclinic crystal system. The computed lattice constant for CaO is a= 4.81 Å which match with the published value (JCPDS File No.37-1497), and for ZnO is a= 3.25 Å b= 5.20 Å which match with the published value (JCPDS File No.036-1451).
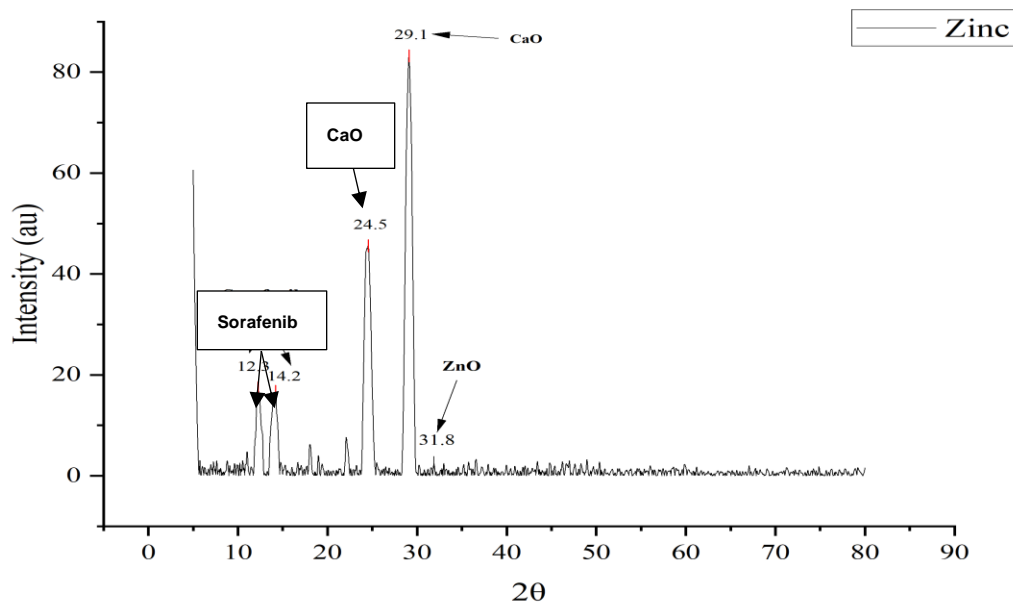
Figure 4.4: X-Ray Diffraction Graph of Zinc Formulated Nano-coated Drug

4.1.3. Fourier Transform Infrared Spectroscopy (FTIR)

To identify potential functional groups contained nano-coated drug, the infrared spectroscopy analysis was conducted. FTIR measurements of the synthesized nano-coated showed absorption bands that were identical to those in the literature. FTIR data of the green copper formulated nano-coated drug showed the peaks at 3912, 3862, 3758, 3690, 3316, 2914, 2862, 2389, 2313, 2111, 1911, 1796, 1639, 1543, 1404, 1296, 1182, 1021, 830, 787 cm^{-1}. The bands between 3900 and 3200 cm^{-1} were attributable to glucoside compound OH stretching vibrations. The polysaccharide -CH$_2$ stretching was responsible for the bands at 2926– 2906 cm^{-1}. The bands at 2380 cm^{-1} were attributable for CO$_2$. The band at 2313 cm^{-1} was assigned to N=C=O. The band at 2111 cm^{-1} was assigned to Alkynes. The bands at 1750–1406 cm–1 were assigned for C=O and C-N stretching. The band at 1543 cm^{-1} was assigned to Aromatic ring of sorafenib drug. The bands at 1300 to 1100 cm^{-1} were attributes for Esters compound. The band at 1021 cm^{-1} was assigned to ethers compound. The band at 830 cm^{-1} indicate the presence of CaO bond, and bond at 787 cm^{-1} indicate the presence of CuO bond.
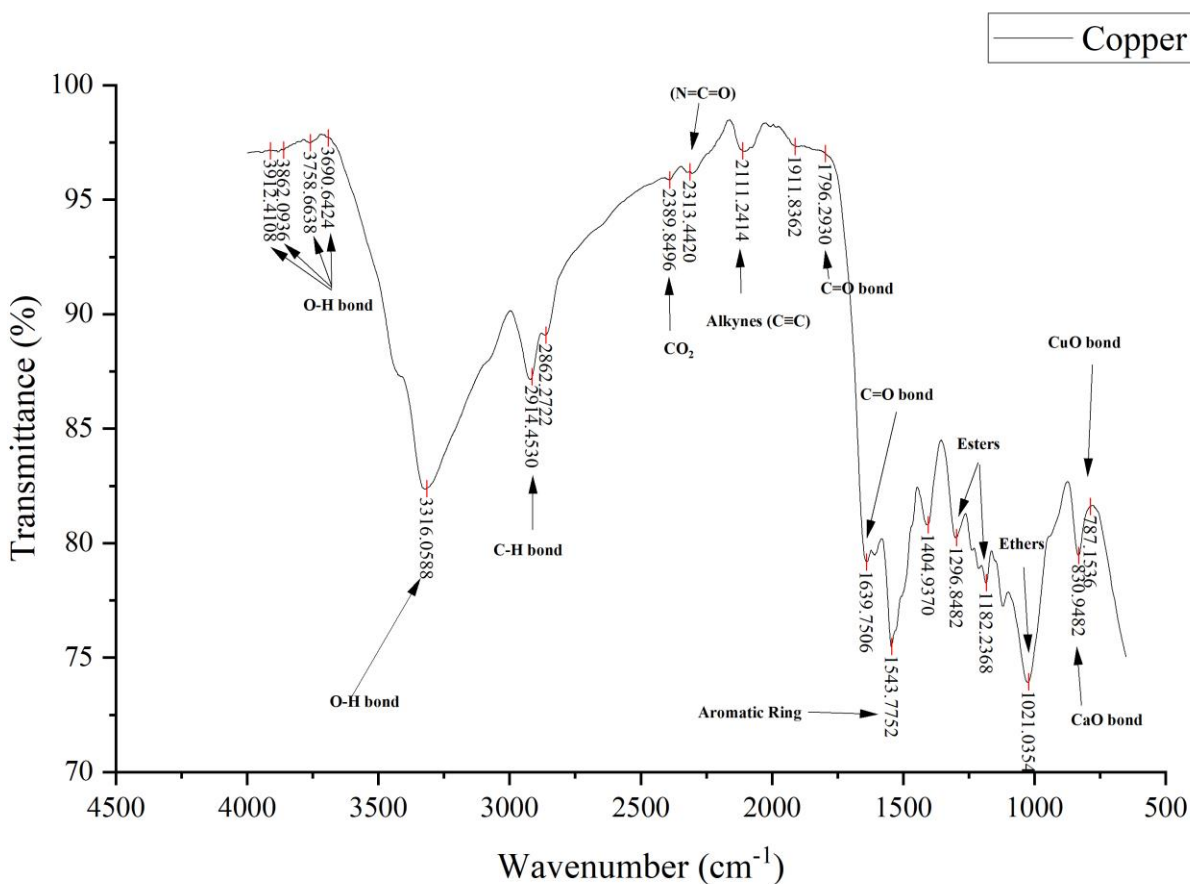
Figure 4.5: FTIR Graph of Copper Formulated Nano-coated Drug

FTIR data of the green zinc formulated nano-coated drug showed the peaks at 3767, 3696, 3289, 2930, 2387, 2302, 2096, 1639, 1548, 1412, 1297, 1183, 1027, 832 cm^{-1}. The bands between 3700 and 3200 cm^{-1} were attributable to glucoside compound OH stretching vibrations. The polysaccharide -CH$_2$ stretching was responsible for the bands at 2926– 2906 cm^{-1}. The bands at 2387 cm^{-1} were attributable for CO$_2$. The band at 2302 cm^{-1} was assigned to N=C=O. The band at 2096 cm^{-1} was assigned to Alkynes. The bands at 1639cm–1 were assigned for C=O and Zn-N stretching. The band at 1548 cm^{-1} was assigned to Aromatic ring of sorafenib drug and ZnN bond between sorafenib and zinc. The bands at 1300 to 1100 cm^{-1} were attributes for Esters compound. The band at 1027 cm^{-1} was assigned to ethers compound, and the band at 832 cm^{-1} indicate the

presence   of   CaO   bond.
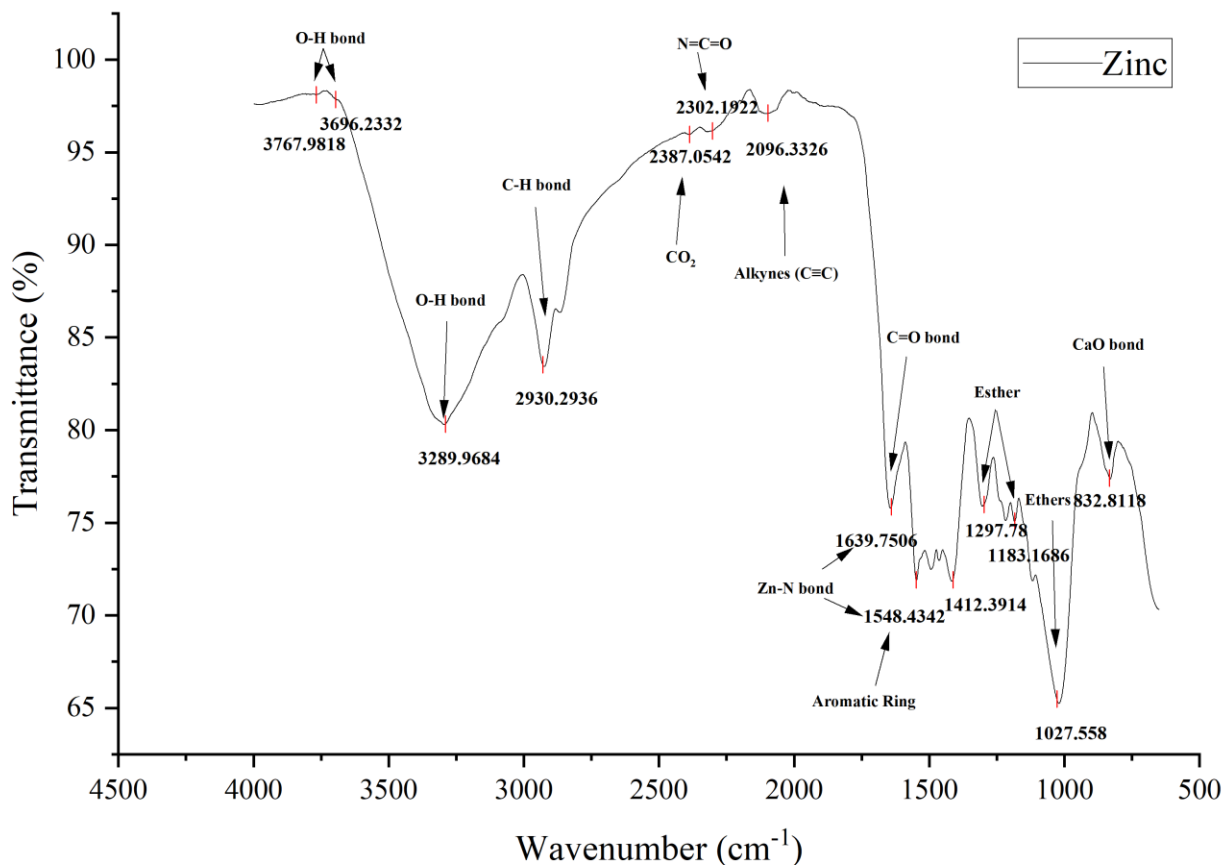
Figure 4.6: FTIR Graph of Zinc Formulated Nano-coated Drug

4.1.4. Scanning Electron Microscopy

SEM was used to analyze the particle size and morphology of green nano-coated drug, and the results are shown in figure below. The surface morphological characteristics were determined and identified using scanning electron microscopy (SEM). The precise measurement regions were chosen at scale bar of 1µm, and 500nm. SEM analysis of copper formulated nano-coated drug were shown in (Figure 4.7A & 4.7B), figure 4.7A indicating good surface coating, good stability, particle size in nanometer, and better surface morphology with red, blue, green, and yellow arrows, and in figure 4.7B the arrows indicate the good coating of calcium nanoparticles. SEM analysis of zinc formulated nano-coated drug were shown in (Figure 4.8A & 4.8B), in figure 4.8A yellow, blue, purple, and green arrows indicates the surface morphology, slight less stability, particle size

and less stable coating of calcium nanoparticles, figure 4.8B indicates that the nano-coated drug is in irregular shape portraying less stable coating.
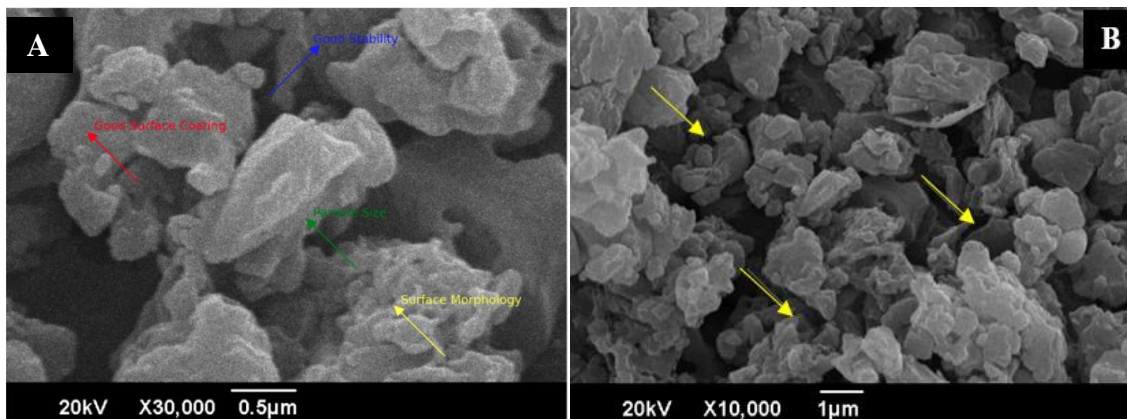
Figure 4.7: SEM image of Copper Formulated Nano-coated drug at different magnifications A) ×30,000 B) ×10,000
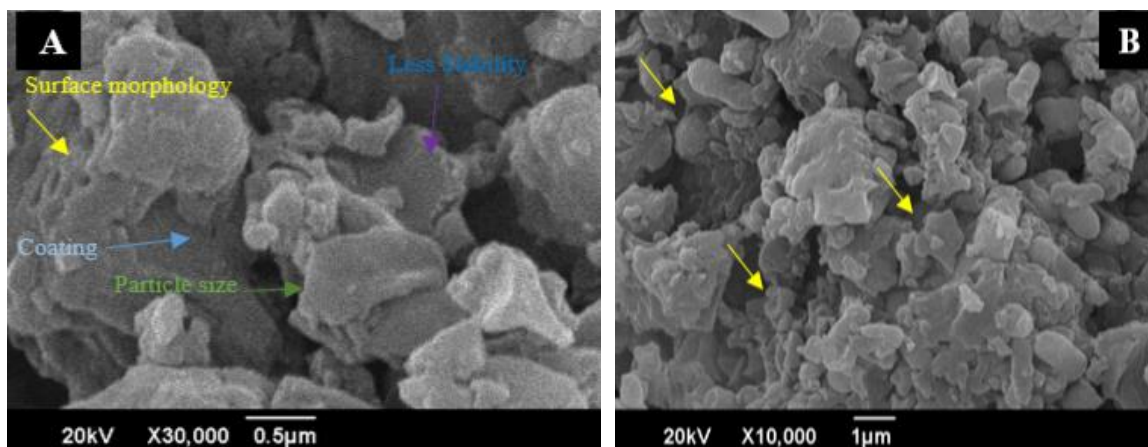
Figure 4.8: SEM image of Zinc Formulated Nano-coated drug at different magnifications A) ×30,000 B) ×10,000

4.1.5. Zeta Analysis

The zeta potential plays an important role in determining the ionic interaction between different molecules and assessing the surface charge of NPs and ultimately the magnitude of electrical double layer repulsion. Zeta potential for biosynthesized nano-coated drugs is shown below in the graph. The nature of surface charge on particles could control the stability of nanoparticles through electrostatic repulsion of particles with each other. The zeta potential for copper ranges from-13.7 or -20.6, for Sorafenib drug -11.5 to -18.1, for Calcium -8.8 to -18.3, and for Zinc -7.45. For copper formulated nano-coated drug, the zeta potential fit values he fit values are seemed more centered

around -18 mV to -21 mV, indicating the presence of all the compounds (sorafenib, copper, and calcium) and through this we can conclude that the copper formulated nano-coated drug is stable. For zinc formulated nano-coated drug, the zeta potential fit values from +12.35 mV to -7.12 mV. The sorafenib value for this was -10mV this is because that it is formulated into nanoparticles and also it is encapsulated in nanoparticles. Fit value ranges indicate that zinc formulated nano-coated drug is also stable but it is slightly less stable than the sample 1 of nano-coated drug. Zeta potential only provides the information towards the surface charge (positive/negative) which can be changed due to various factors such as pH, ionic strength, and concentration. Therefore, it should never be associated with measuring charge or charge density as it is variable. The only important thing to focus on is the magnitude, the higher the value of magnitude, the more stable the colloidal suspension.

Table 4.1: Raw and Fit Zeta Potential Values of Copper Formulated Nano-coated Drug

#	Valid	Raw		Fit			
		μ	ζ	μ	σ	ζ	σ
		(μm.cm/V.s)	(mV)	(μm.cm/V.s)		(mV)	
Avg		0.18	2.37	0.09	1.58	1.12	20.28
1	✓	-0.55	-7.1	-0.48	-1.77	-6.17	-22.73
2	✓	-0.28	-3.55	-0.06	-1.53	-0.75	-19.67
3	✓	1.38	17.76	0.8	-1.43	10.26	-18.44
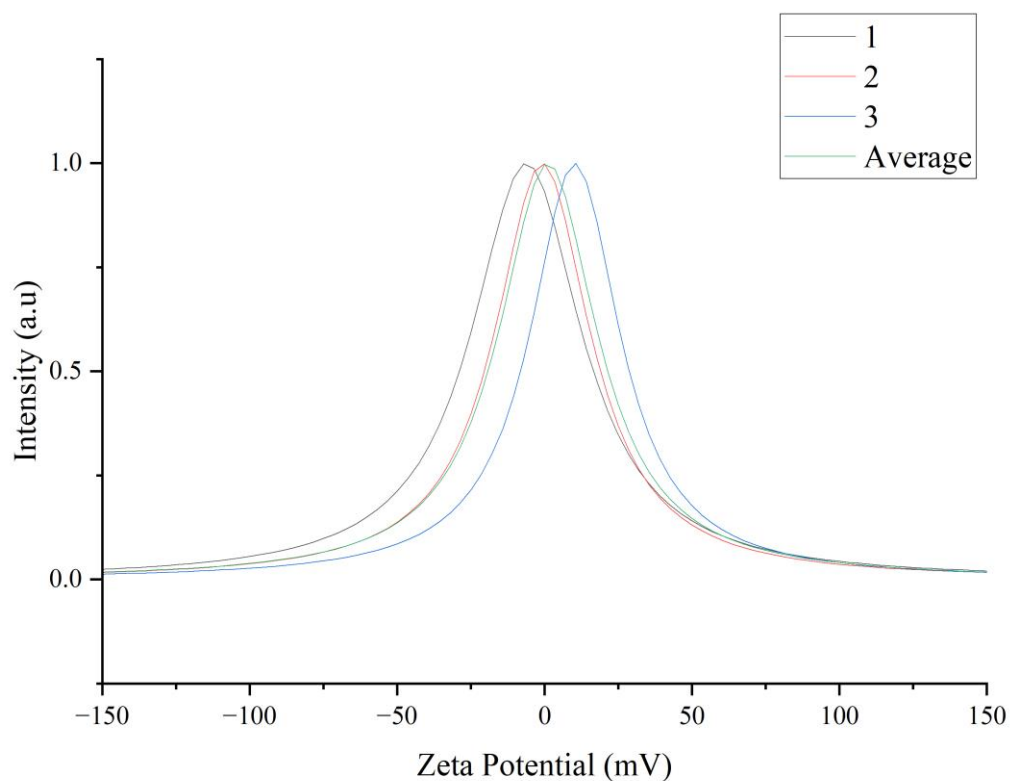
Figure 4.9: Zeta Potential Result of Copper Formulated Nano-coated Drug

Table 4.2: Raw and Fit Zeta Potential Values of Zinc Formulated Nano-coated Drug

#	Valid	Raw		Fit			
		μ	ζ	μ	σ	ζ	σ
		(μm.cm/V.s)	(mV)	(μm.cm/V.s)		(mV)	
Avg		-0.84	-10.8	0.85	0.56	-10.98	7.24
1	✓	-0.78	-9.97	-0.88	-0.57	-11.32	-7.34
2	✓	-0.97	-12.47	-0.8	-0.57	-10.29	-7.26
3	✓	-0.78	-9.97	-0.88	-0.55	-11.32	-7.12
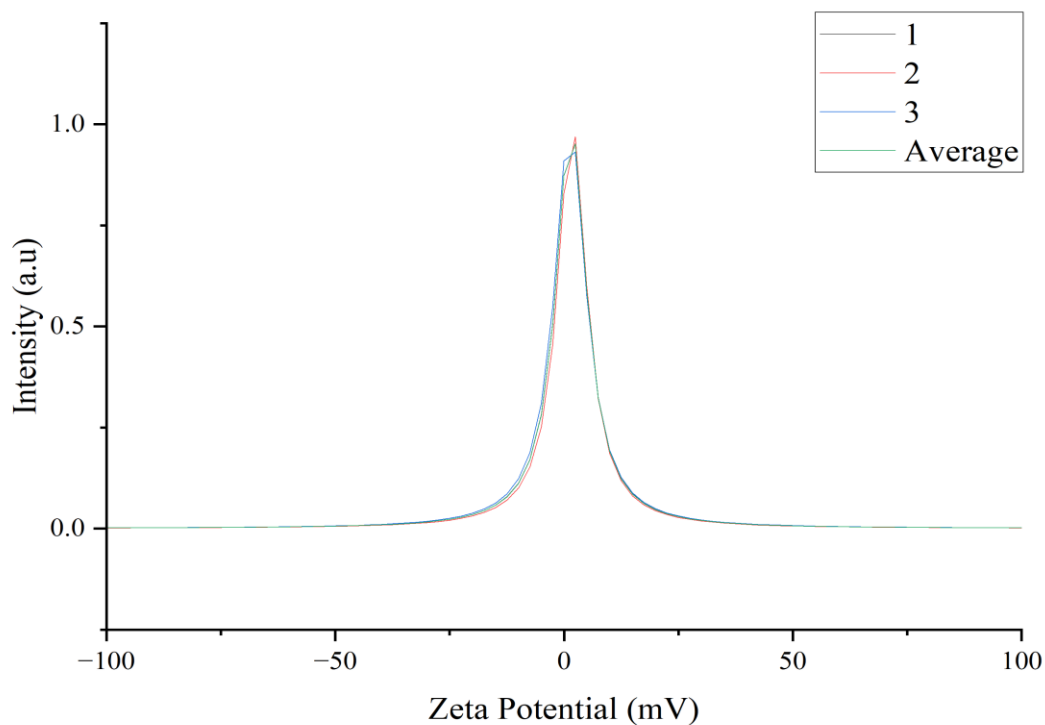
Figure 4.10: Zeta Potential Result of Zinc Formulated Nano-coated Drug

4.1.6. *Dynamic Light Scattering (DLS)*

The nano-coated samples were prepared and particle sizes was measured using the dynamic light scattering technique. In DLS technique, the size measured was the theoretical sphere's hydrodynamic diameter that scatters with the same speed as nanoparticle.

The results obtained for the samples 1–2 are shown in Figure. Analyses of obtained results indicate that in the investigated nano-coated drug with size 13-14nm (0.013-0.014 μm) and 11-12 nm (0.011-0.012 μm).
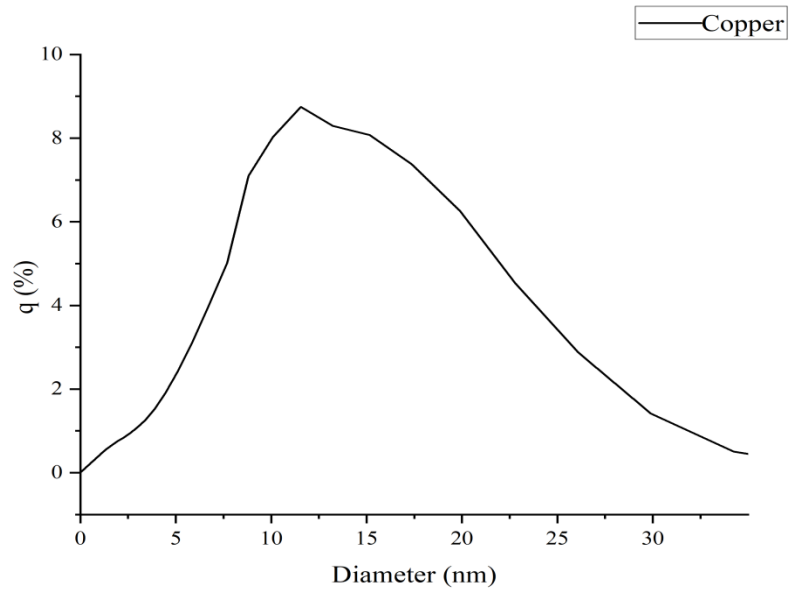
Figure 4.11: DLS Graph of Copper Formulated Nano-coated Drug
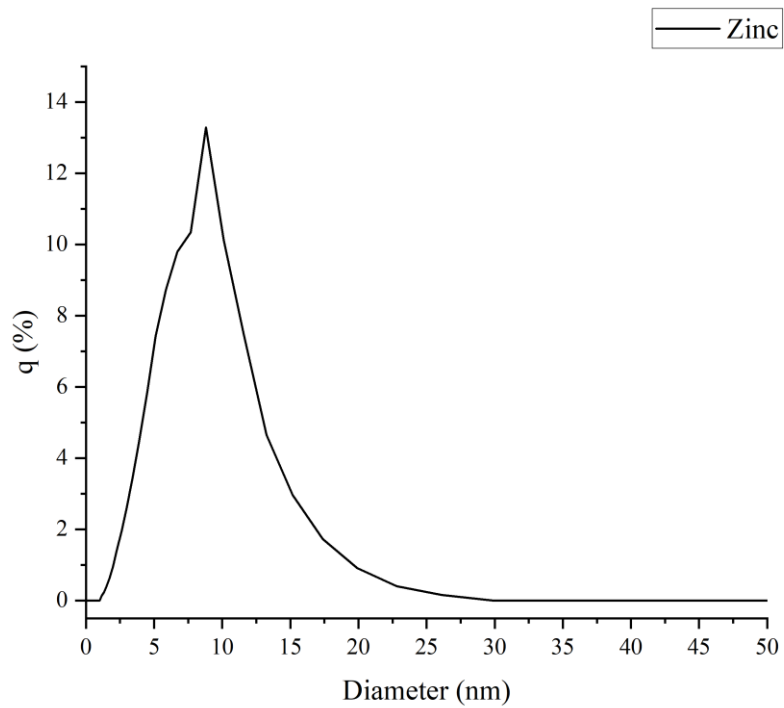
Figure 4.12: DLS Graph of Zinc Formulated Nano-coated Drug

4.2.Anticancer activity

In vitro cytotoxicity of the nano-coated drug of both samples was evaluated against MCF-7 breast cancer cell lines. For this purpose, MCF-7 cells were exposed to with three groups 1 drug and 2 nano-coated samples (first copper nanoparticle + sorafenib + calcium nanoparticle, second zinc nanoparticle + sorafenib + calcium nanoparticle) at concentration (50 for drug, and 100 µg/ml for both nano-coated drug samples) for 24 h. According to the results of cell viability using MTT assay, both nano-coated drug indicated the good anticancer activities against only the drug sample.

Table 4.3: Groups vs Cell Viability Anti-cancer Activity

Groups	Cell Viability (%)
Control	100
Sorafenib	89.8
Copper Formulated Nano-coated Drug	64.8
Zinc Formulated Nano-coated Drug	68.5
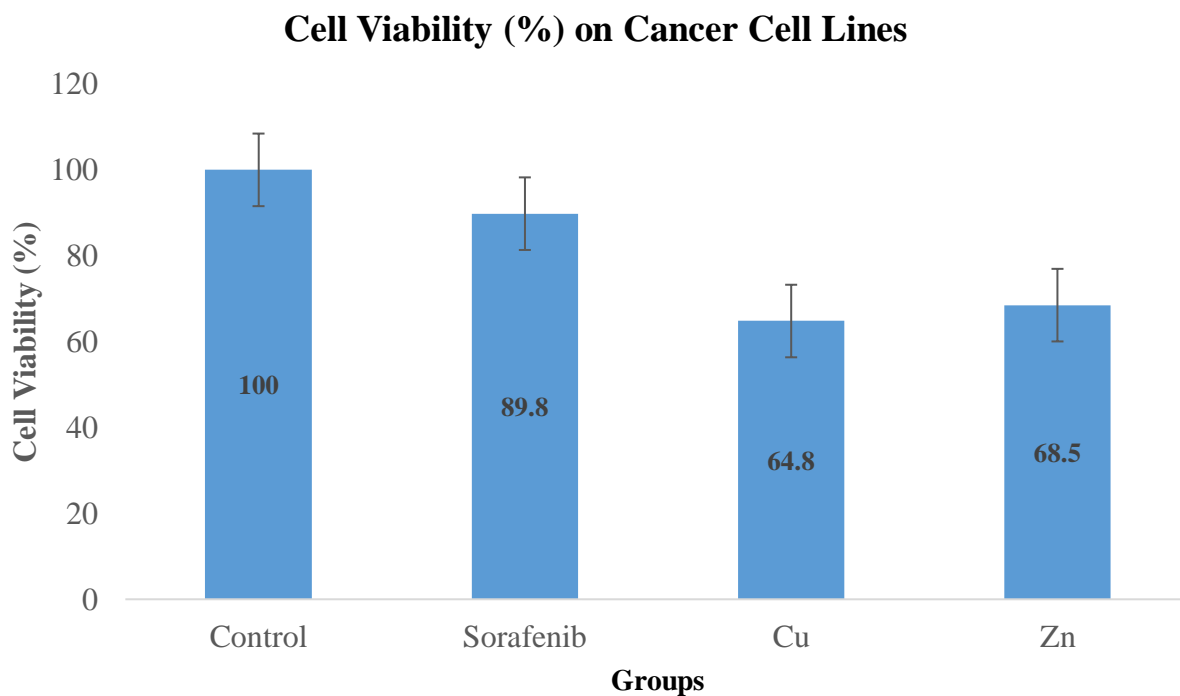
Figure 4.13: Cell Viability (%) on Cancer Cell Lines

4.2.1. IC$_{50}$ Values:

IC$_{50}$ value of all the compound drug, Copper Formulated& Zinc Formulated nano-coated drug was calculated using Graph pad prism 9. The calculated sorafenib IC$_{50}$ values was 7.104µM, Copper Formulated nano-coated drug have IC$_{50}$ value of 4.599µM, and Zinc Formulated nano-coated drug have IC$_{50}$ values of 34.50µM.

CHAPTER 5: DISCUSSION

Cancer is a group of diseases characterized by uncontrolled cell growth and the potential to invade or spread to other parts of the body. Unlike normal cells, cancer cells ignore signals to stop dividing, evade apoptosis (programmed cell death), and can grow indefinitely. This malignant transformation results from genetic mutations and epigenetic changes. There are over 100 types of cancer, each classified based on the origin of the malignant cells (Yadav *et al*., 2020). These include carcinomas (epithelial cells), sarcomas (connective tissue), leukemia (blood-forming tissues), and lymphomas (immune system). Cancer's heterogeneity and adaptability make it a challenging disease to diagnose, treat, and cure (Kumari *et al*., 2020).

Cancer can be caused by a variety of factors, often categorized into genetic and environmental causes. Genetic predisposition plays a role in some cancers due to inherited mutations. Environmental factors include exposure to carcinogens such as tobacco smoke, radiation, chemicals, and certain infections (e.g., HPV, hepatitis B and C). Lifestyle factors like diet, physical inactivity, and alcohol consumption also contribute. The interplay between these factors and genetic susceptibility leads to DNA damage and mutations that drive cancer progression (Yasmin *et al*., 2021).

Cancer diagnosis involves a combination of clinical evaluation, imaging, laboratory tests, and histopathological examination. Initial symptoms and physical examinations guide the use of diagnostic imaging techniques such as X-rays, CT scans, MRI, and PET scans to locate tumors. Laboratory tests including blood tests and tumor markers help in identifying abnormalities. Definitive diagnosis is typically achieved through biopsy, where a tissue sample is examined microscopically for malignant cells. Molecular diagnostic tests, such as genetic profiling, provide additional information on specific mutations and can guide targeted therapies (Lind *et al*., 1989).

Cancer treatment depends on the type, location, stage, and genetic profile of the disease. Standard treatment modalities include surgery, radiation therapy, chemotherapy, immunotherapy, and targeted therapy. Surgery aims to remove localized tumors, while radiation therapy uses high-energy rays to kill cancer cells. Chemotherapy employs cytotoxic drugs to target rapidly dividing cells. Immunotherapy enhances the body's immune response against cancer, and targeted therapy uses drugs designed to specifically attack cancer cell markers. Combination therapies are often employed to improve efficacy and reduce the risk of resistance (Tewari *et al*., 2022).

Human cell lines are cultures of human cells that can proliferate indefinitely in vitro. These cell lines are derived from various tissues and are used extensively in biomedical research to study cellular functions, disease mechanisms, and drug responses. They provide a consistent, reproducible, and controllable environment for experiments. Cell lines like HeLa (cervical cancer), HEK293 (kidney), MCF-7 (breast cancer), A549 (lung cancer), HCT116 (colorectal cancer), and U87 (glioblastoma) are some examples. They play a crucial role in cancer research, enabling the study of cancer biology, screening of anticancer drugs, and understanding mechanisms of drug resistance (Kashyap *et al.*, 2011).

Bacopa monnieri, commonly known as Brahmi, is a traditional medicinal herb used in Ayurvedic medicine. It is known for its neuroprotective properties and is used to enhance memory, cognition, and reduce anxiety. Recent studies have shown that Bacopa monnieri also possesses anticancer properties. It contains bioactive compounds such as bacosides, which have been found to induce apoptosis and inhibit the proliferation of cancer cells. The herb has shown potential in modulating various molecular pathways involved in cancer progression, making it a candidate for complementary cancer therapy (Banerjee *et al.*, 2021). Additionally, its anti-inflammatory and immunomodulatory properties contribute to its anticancer effects. Bacopa monnieri is being investigated for its potential to be developed into an adjunct therapy for various cancers, offering a natural, less toxic alternative to synthetic drugs (Ghosh *et al.*, 2021).

Nanoparticles are tiny particles with dimensions measured in nanometers. Due to their small size, large surface area, and unique physical and chemical properties, nanoparticles are used in various fields, including medicine (Nikzamir *et al.*, 2021). In cancer treatment, nanoparticles can be engineered to deliver drugs directly to tumor cells, improving the efficacy and reducing the side effects of conventional chemotherapy. They can also be used for imaging and diagnostic purposes. Types of nanoparticles used in cancer therapy include liposomes, polymeric nanoparticles, dendrimers, and metal nanoparticles like gold and silver (S. Khan *et al.*, 2022). They enhance the solubility and stability of drugs, allowing for controlled and targeted drug delivery. This reduces the required dosage and minimizes systemic toxicity, leading to fewer side effects. Nanoparticles can be functionalized with ligands to target specific cancer cell markers, improving the selectivity and efficacy of the treatment. Additionally, they can overcome multidrug resistance by facilitating drug delivery through different mechanisms (Dolai *et al.*, 2021).

UV analysis of nano-coated drug was done to check the drug loading using UV-Spectrophotometry (Barbosa *et al*., 2017). From the literature, we checked that the drug absorbance is shown as 260-270nm. From the given below results we can checked and characterized that the drug was absorbed by both the samples. In copper formulated nano-coated drug the maximum absorbance peak was shown on 262nm and in zinc formulated nano-coated drug the maximum absorbance peak was shown at 263nm. The Ca-O bond shows that peaks at 210-250nm, Cu-O shows peaks at 280-350nm, and Zn-O shows peaks at 300-350nm

An X-ray diffractometer was used to validate the occurrence of NPs and to examine their structural characteristics. X-ray diffraction technique was adopted for determining the crystalline structure and phase purity of green nano-composite (H. Khan *et al*., 2020). The data, according to X-ray diffraction technique, is most likely crystalline nature of the composite indicating the production of nano-coated drug. Presence of nano-coated drug peaks in a single pattern.

Scanning electron microscopy (SEM) was used to analyze the particle size and morphology of green nano-drug. The SEM photomicrograph of nano-drug revealed a wide range of size distribution (Odziomek *et al*., 2016). The result of copper formulated nano-coated drug indicates that it is good stable, have particle size less than 100nm, have excellent surface morphology, and excellent coated in calcium nanoparticles. The results of zinc formulated nano-coated drug indicates that it less stable than the copper formulated nano-coated drug, are irregular in shape, have size smaller than 100nm, but are not perfectly coated in calcium nanoparticles. To obtain the more accurate size of the both nano-coated drugs the dynamic light scattering test was performed.

FTIR spectroscopy was used to determine the functional groups involved in the production of green nano-drug. FTIR measurements of the synthesized nano-catalyst showed absorption bands that were identical to those in the aqueous extract (Eid *et al*., 2022). FTIR data of the both green nano-coated drug showed the bands at 3912, 3862, 3758, 3690, 3316, 2914, 2862, 2389, 2313, 2111, 1911, 1796, 1639, 1543, 1404, 1296, 1182, 1021, 830, 787 cm^{-1}. The bands between 3900 and 3200 cm^{-1} were attributable to glucoside compound OH stretching vibrations. According to (Keijok *et al*., 2019), the polysaccharide -CH$_2$ stretching was responsible for the bands at 2926–2906 cm^{-1}. The bands at 2380 cm^{-1} were attributable for CO_2. The band at 2313 cm^{-1} was assigned to N=C=O. The band at 2111 cm^{-1} was assigned to Alkynes. According to (Jyoti *et al*., 2016), the bands at 1750–1406 cm–1 were assigned for C=O and C-N stretching. The bands at 1639cm–1

were assigned for C=O and Zn-N stretching. The band at 1548 cm^{-1} was assigned to Aromatic ring of sorafenib drug and ZnN bond between sorafenib and zinc. The bands at 1300 to 1100 cm^{-1} were attributes for Esters compound. The band at 1021 cm^{-1} was assigned to ethers compound. The band at 830 cm^{-1} indicate the presence of CaO bond, and bond at 787 cm^{-1} indicate the presence of CuO bond.

Zeta size analysis showed that the size of nanoparticles, in this 1 mL syringe we utilized for drop-wise addition of nano-drug (Hafezi *et al*., 2021). The zeta potential for copper ranges from -13.7 or -20.6mV, for Sorafenib drug -11.5 to -18.1mV, for Calcium -8.8 to -18.3mV, and for Zinc -7.45mV. For copper formulated nano-coated drug, the zeta potential fit values he fit values are seemed more centered around -18 mV to -21 mV, indicating the presence of all the compounds (sorafenib, copper, and calcium) and through this we can conclude that the copper formulated nano-coated drug is stable. For zinc formulated nano-coated drug, the zeta potential fit values from -12.35 mV to -7.12 mV. The sorafenib value for this was -10mV this is because that it is formulated into nanoparticles and also it is encapsulated in nanoparticles.

Dynamic light scattering also known as quasi-elastic light scattering or photon correlation spectroscopy. It is used to measure the particles size distribution in suspension. The analysis is done was the when the light scattered from a laser and passes through the sample (Goldburg *et al*., 1999). It provides the information about the aggregation and stability of sample and also about the particle size distribution, obtained results indicate that in the investigated nano-coated drug with size 13-14nm (0.013-0.014 μm) and 11-12 nm (0.011-0.012 μm).

MTT assay was used to check anticancer activity, both nan-coated drugs were treated on MCF-7 cell lines, according to results which were obtain the copper formulated nano-coated drug showed the 64.8% cell viability, followed by zinc formulated nano-coated drug (68.5%) and then the sorafenib drug (89.8%), meaning that the samples used were have the anti-cancerous activity higher than the sorafenib drug. It was concluded that we can use the nano-coated drug in future to treatment the patients with cancer.

Green Synthesis of nano-coated drugs and their validation through various characterization techniques as well its significant cytotoxic testing on MCF-7 cell lines proved that these can be used for the delivery of anticancerous drug and could be used as a modality for cancer therapy.

CHAPTER 6: CONCLUSION AND FUTURE PROSPECTIVE

The future of using metal nanoparticles to enhance the sorafenib activity against cancerous cell lines holds significant promise for advancing cancer treatment. As research progresses, there is potential to develop highly sophisticated nanoparticle formulations that optimize the delivery and efficacy of sorafenib, minimizing its side effects and overcoming drug resistance mechanisms. Future studies will likely focus on tailoring the physical and chemical properties of these nanoparticles to improve targeting specificity, ensuring that sorafenib is delivered precisely to cancer cells while sparing healthy tissues. Additionally, the development of multifunctional nanoparticles that combine therapeutic delivery with diagnostic capabilities could enable real-time monitoring of treatment response. The integration of personalized medicine approaches, leveraging genetic and molecular profiling of tumors, will further enhance the effectiveness of these treatments. Clinical trials and extensive safety evaluations will be critical in translating these innovations from the laboratory to clinical practice, potentially leading to more effective and less toxic cancer therapies

The integration of metal nanoparticles with sorafenib represents a groundbreaking advancement in cancer therapy, offering significant improvements in drug delivery, efficacy, and safety. By harnessing the unique properties of metal nanoparticles, such as their high surface area and ability to be functionalized for targeted delivery, researchers have opened new avenues for enhancing the therapeutic potential of sorafenib. According to results, it was observed that the drug was absorbed, and was excellent coated in nanoparticle making it beneficial for drug delivery. According to FTIR, the every bond of drug and nanoparticles were present. And through DLS, and Zeta potential, it is concluded that nano-coated drugs were in size of 10nm-15nm and were stable. In the end, the anticancer activity of nano-coated drug indicate that the samples have the good excellent activity than the actual sorafenib drug and can be used in future on animal model and then the clinical trials.

REFERENCES

➢ Abad, S.-A., Arezzo, A., Homer-Vanniasinkam, S., & Wurdemann, H. A. (2022). Soft robotic systems for endoscopic interventions. In *Endorobotics* (pp. 61-93): Elsevier.

➢ Abdul Manap, A. S., Vijayabalan, S., Madhavan, P., Chia, Y. Y., Arya, A., Wong, E. H., . . . Koshy, S. J. D. t. i. (2019). Bacopa monnieri, a neuroprotective lead in Alzheimer disease: a review on its properties, mechanisms of action, and preclinical and clinical studies. *13*, 1177392819866412.

➢ Aguiar, S., & Borowski, T. J. R. r. (2013). Neuropharmacological review of the nootropic herb Bacopa monnieri. *16*(4), 313-326.

➢ Ali, F., Hussain, S., Memon, S. A., & Iqbal, S. S. J. D. S. A. H. M. J. (2023). Recently top trending cancers in a tertiary cancer hospital in Pakistan. *5*(2), 42-49.

➢ Ando, Y., Zhao, X. J. N. d., & technology, f. c. (2006). Synthesis of carbon nanotubes by arc-discharge method. *16*(3), 123-138.

➢ Azim, H. A., Omar, A., Atef, H., Zawahry, H., Shaker, M. K., Abdelmaksoud, A. K., . . . Kassem, L. J. J. o. h. c. (2018). Sorafenib plus tegafur–uracil (UFT) versus sorafenib as first line systemic treatment for patients with advanced stage HCC: a phase II trial (ESLC01 study). 109-119.

➢ Banerjee, S., Anand, U., Ghosh, S., Ray, D., Ray, P., Nandy, S., . . . Dey, A. J. P. R. (2021). Bacosides from Bacopa monnieri extract: An overview of the effects on neurological disorders. *35*(10), 5668-5679.

➢ Barbosa, F., Rodrigues, V., Volpato, N., Schapoval, E., Steppe, M., Garcia, C., & Mendez, A. (2017). UV SPECTROPHOTOMETRIC METHOD FOR QUANTITATIVE DETERMINATION OF AGOMELATINE IN COATED TABLETS. *Drug Analytical Research, 1*, 24-29. doi:10.22456/2527-2616.79219

➢ Basque, J. R., Chénard, M., Chailler, P., & Ménard, D. J. J. o. c. b. (2001). Gastric cancer cell lines as models to study human digestive functions. *81*(2), 241-251.

➢ Behranvand, N., Nasri, F., Zolfaghari Emameh, R., Khani, P., Hosseini, A., Garssen, J., & Falak, R. J. C. i., immunotherapy. (2022). Chemotherapy: a double-edged sword in cancer treatment. *71*(3), 507-526.

➢ Bhardwaj, N., & Kundu, S. C. J. B. a. (2010). Electrospinning: A fascinating fiber fabrication technique. *28*(3), 325-347.

➢ Bokov, D., Turki Jalil, A., Chupradit, S., Suksatan, W., Javed Ansari, M., Shewael, I. H., . . . engineering. (2021). Nanomaterial by sol-gel method: synthesis and application. *2021*(1), 5102014.

➢ Bray, F., Laversanne, M., Sung, H., Ferlay, J., Siegel, R. L., Soerjomataram, I., & Jemal, A. (2024). Global cancer statistics 2022: GLOBOCAN estimates of incidence and mortality worldwide for 36 cancers in 185 countries. *74*(3), 229-263. doi:https://doi.org/10.3322/caac.21834

➢ Brimson, J. M., Prasanth, M. I., Plaingam, W., Tencomnao, T. J. J. o. t., & medicine, c. (2020). Bacopa monnieri (L.) wettst. Extract protects against glutamate toxicity and increases the longevity of Caenorhabditis elegans. *10*(5), 460-470.

➢ Bruckner, J. R., Bauhof, J., Gebhardt, J., Beurer, A.-K., Traa, Y., & Giesselmann, F. J. T. J. o. P. C. B. (2021). Mechanisms and intermediates in the true liquid crystal templating synthesis of mesoporous silica materials. *125*(12), 3197-3207.

➢ Burnham, J. C. J. B. o. t. H. o. M. (1989). American physicians and tobacco use: two surgeons general, 1929 and 1964. *63*(1), 1-31.

➢ Caracciolo, G., Vali, H., Moore, A., & Mahmoudi, M. J. N. T. (2019). Challenges in molecular diagnostic research in cancer nanotechnology. *27*, 6-10.

➢ Castro, L., Blázquez, M. L., Muñoz, J. A., González, F., & Ballester, A. J. I. n. (2013). Biological synthesis of metallic nanoparticles using algae. *7*(3), 109-116.

➢ Cervello, M., Bachvarov, D., Lampiasi, N., Cusimano, A., Azzolina, A., McCubrey, J. A., & Montalto, G. J. C. c. (2012). Molecular mechanisms of sorafenib action in liver cancer cells. *11*(15), 2843-2855.

➢ Chae, Y. K., Pan, A. P., Davis, A. A., Patel, S. P., Carneiro, B. A., Kurzrock, R., & Giles, F. J. J. M. c. t. (2017). Path toward precision oncology: review of targeted therapy studies and tools to aid in defining "actionability" of a molecular lesion and patient management support. *16*(12), 2645-2655.

➢ Chai, C., Tang, H., Yi, J., Li, L., Yu, C., Su, Y., . . . Luo, W. J. H. C. (2024). Establishment and characterization of DPC-X4: a novel mixed-type ampullary cancer cell line. *37*(2), 531-545.

➢ Chandra, R. A., Keane, F. K., Voncken, F. E., & Thomas, C. R. J. T. L. (2021). Contemporary radiotherapy: present and future. *398*(10295), 171-184.

➢ Chen, H., Kuhn, J., Lamborn, K. R., Abrey, L. E., DeAngelis, L. M., Lieberman, F., . . . Drappatz, J. J. N.-O. A. (2020). Phase I/II study of sorafenib in combination with erlotinib for recurrent glioblastoma as part of a 3-arm sequential accrual clinical trial: NABTC 05-02. *2*(1), vdaa124.

➢ Cheng, A.-L., Guan, Z., Chen, Z., Tsao, C.-J., Qin, S., Kim, J. S., . . . Yu, S. J. E. J. o. C. (2012). Efficacy and safety of sorafenib in patients with advanced hepatocellular carcinoma according to baseline status: Subset analyses of the phase III Sorafenib Asia–Pacific trial. *48*(10), 1452-1465.

➢ Cheng, Z., Wei-Qi, J., & Jin, D. J. B. e. B. A.-R. o. C. (2020). New insights on sorafenib resistance in liver cancer with correlation of individualized therapy. *1874*(1), 188382.

➢ Chryssafidis, P., Tsekouras, A. A., & Macheras, P. J. P. R. (2021). Revising pharmacokinetics of oral drug absorption: II bioavailability-bioequivalence considerations. *38*, 1345-1356.

➢ Ciriminna, R., Fidalgo, A., Pandarus, V., Beland, F., Ilharco, L. M., & Pagliaro, M. J. C. r. (2013). The sol–gel route to advanced silica-based materials and recent applications. *113*(8), 6592-6620.

➢ Coriat, R., Nicco, C., Chéreau, C., Mir, O., Alexandre, J., Ropert, S., . . . Batteux, F. J. M. c. t. (2012). Sorafenib-induced hepatocellular carcinoma cell death depends on reactive oxygen species production in vitro and in vivo. *11*(10), 2284-2293.

➢ Correa, N. M., Silber, J. J., Riter, R. E., & Levinger, N. E. J. C. R. (2012). Nonaqueous polar solvents in reverse micelle systems. *112*(8), 4569-4602.

➢ Cowan, A. J., Green, D. J., Kwok, M., Lee, S., Coffey, D. G., Holmberg, L. A., . . . Libby, E. N. J. J. (2022). Diagnosis and management of multiple myeloma: a review. *327*(5), 464-477.

➢ Cozzi, E., Bosio, E., Seveso, M., Vadori, M., & Ancona, E. J. B. m. b. (2005). Xenotransplantation—current status and future perspectives. *75*(1), 99-114.

➢ Creighton, J., & Ho, P. J. A. I. (2001). Introduction to chemical vapor deposition (CVD). *407*.

➤ Dai, X., Cheng, H., Bai, Z., & Li, J. J. J. o. C. (2017). Breast cancer cell line classification and its relevance with breast tumor subtyping. *8*(16), 3131.

➤ Daigeler, A., Druecke, D., Hakimi, M., Duchna, H.-W., Goertz, O., Homann, H.-H., . . . Steinau, H.-U. J. L. s. a. o. s. (2009). Reconstruction of the thoracic wall—long-term follow-up including pulmonary function tests. *394*, 705-715.

➤ Das, U. N., & Das, U. N. J. M. B. A. o. C. (2020). Introduction to Genes, Oncogenes, and Anti-oncogenes. 1-40.

➤ Davey, M. G., Miller, N., & McInerney, N. M. J. C. (2021). A review of epidemiology and cancer biology of malignant melanoma. *13*(5).

➤ Deshpande, V., & Iafrate, A. J. J. D. p. o. i. d. (2018). General principles in the diagnosis of infection. 3.

➤ Devi, P. U. J. H. A. (2004). Basics of carcinogenesis. *17*(1), 16-24.

➤ Dolai, J., Mandal, K., & Jana, N. R. J. A. A. N. M. (2021). Nanoparticle size effects in biomedical applications. *4*(7), 6471-6496.

➤ Duffy, M. J., O'Grady, S., Tang, M., & Crown, J. J. C. t. r. (2021). MYC as a target for cancer treatment. *94*, 102154.

➤ Eid, M. (2022). Characterization of Nanoparticles by FTIR and FTIR-Microscopy. In.

➤ Enteropathica, A., Albinism, A., Albinism, A., Hereditary, A. O. J. D. I. S. G., & Review, C. B. (2017). 11.1 GENETIC DISEASES. 402.

➤ Fahrner, W. R. (2005). *Nanotechnology and nanoelectronics: materials, devices, measurement techniques*: Springer.

➤ Farshi, E. (2024). Comprehensive Overview Of 31 Types Of Cancer: Incidence, Categories, Treatment Options, And Survival Rates. *Journal of Gastroenterology and Hepatology*.

➤ Ferrari, M. T. M., Elias, F. M., Gomes, N. L. R. A., Batista, R. L., Faria Jr, J. A. D., Nishi, M. Y., . . . Science, M. (2023). WT1: A single gene associated with multiple and severe phenotypes. 100143.

➤ Franks, L. M., & Teich, N. M. (1997). *Introduction to the cellular and molecular biology of cancer*: Oxford University Press.

➤ Galle, P. R., Dufour, J.-F., Peck-Radosavljevic, M., Trojan, J., & Vogel, A. J. F. O. (2021). Systemic therapy of advanced hepatocellular carcinoma. *17*(10), 1237-1251.

➢ Gan, Y. X., Jayatissa, A. H., Yu, Z., Chen, X., & Li, M. J. J. o. N. (2020). Hydrothermal synthesis of nanomaterials. *2020*.

➢ Ganjewala, D., & Srivastava, A. K. J. M. A. P. S. B. (2011). Recent progress on chemical composition and bioactivities of Bacopa monnieri (Linn.) a plant of Ayurveda. *5*, 102-108.

➢ Gazdar, A. F., Girard, L., Lockwood, W. W., Lam, W. L., & Minna, J. D. J. J. o. t. N. C. I. (2010). Lung cancer cell lines as tools for biomedical discovery and research. *102*(17), 1310-1321.

➢ Ghosh, S., Khanam, R., Acharya Chowdhury, A. J. N., & Cancer. (2021). The evolving roles of Bacopa monnieri as potential anti-cancer agent: a review. *73*(11-12), 2166-2176.

➢ Goldburg, W. I. J. A. J. o. P. (1999). Dynamic light scattering. *67*(12), 1152-1160.

➢ Goodspeed, A., Heiser, L. M., Gray, J. W., & Costello, J. C. J. M. C. R. (2016). Tumor-derived cell lines as molecular models of cancer pharmacogenomics. *14*(1), 3-13.

➢ Grassin-Delyle, S., Semeraro, M., Lamy, E., Urien, S., Runge, I., Foissac, F., . . . Roberts, I. J. B. J. o. A. (2022). Pharmacokinetics of tranexamic acid after intravenous, intramuscular, and oral routes: a prospective, randomised, crossover trial in healthy volunteers. *128*(3), 465-472.

➢ Guérit, E., Arts, F., Dachy, G., Boulouadnine, B., Demoulin, J.-B. J. C., & Sciences, M. L. (2021). PDGF receptor mutations in human diseases. *78*, 3867-3881.

➢ Hafezi, R. (2021). Formulation and characterization of oxims loaded PLGA nanoparticles.

➢ Harish, V., Ansari, M., Tewari, D., Yadav, A. B., Sharma, N., Bawarig, S., . . . Barhoum, A. J. J. o. t. T. I. o. C. E. (2023). Cutting-edge advances in tailoring size, shape, and functionality of nanoparticles and nanostructures: A review. *149*, 105010.

➢ Hasan, A., Rizvi, S. F., Parveen, S., Pathak, N., Nazir, A., & Mir, S. S. (2022). Crosstalk Between ROS and Autophagy in Tumorigenesis: Understanding the Multifaceted Paradox. *Front Oncol, 12*, 852424. doi:10.3389/fonc.2022.852424

➢ Hatton, I. A., Galbraith, E. D., Merleau, N. S., Miettinen, T. P., Smith, B. M., & Shander, J. A. J. P. o. t. N. A. o. S. (2023). The human cell count and size distribution. *120*(39), e2303077120.

➢ Hench, L. L., & West, J. K. J. C. r. (1990). The sol-gel process. *90*(1), 33-72.

➢ Hill, B. T. J. C. O. O. B. P. (2019). Etiology of cancer. 11-17.

➢ Horwitz, K. B., & Sartorius, C. A. J. J. o. m. e. (2020). 90 years of progesterone: progesterone and progesterone receptors in breast cancer: past, present, future. *65*(1), T49-T63.

➢ Hosseinzadeh, F., Ai, J., Hajifathali, A., Muhammadnejad, S., Ebrahimi-Barough, S., Seyhoun, I., . . . Ahmadpour, S. J. P. R. (2022). The effects of Sorafenib and Natural killer cell co-injection in combinational treatment of hepatocellular carcinoma; an in vivo approach. *74*(2), 379-391.

➢ Hsu, C.-H., Shen, Y.-C., Shao, Y.-Y., Hsu, C., & Cheng, A.-L. J. J. o. h. c. (2014). Sorafenib in advanced hepatocellular carcinoma: current status and future perspectives. 85-99.

➢ Hutchinson, J., & Evans, A. J. A. m. (2000). Mechanics of materials: top-down approaches to fracture. *48*(1), 125-135.

➢ Infanger, D. W., Lynch, M. E., & Fischbach, C. J. A. r. o. b. e. (2013). Engineered culture models for studies of tumor-microenvironment interactions. *15*(1), 29-53.

➢ Ingale, A. G., & Chaudhari, A. J. J. N. N. (2013). Biogenic synthesis of nanoparticles and potential applications: an eco-friendly approach. *4*(165), 1-7.

➢ Iravani, S. J. G. c. (2011). Green synthesis of metal nanoparticles using plants. *13*(10), 2638-2650.

➢ Ishihara, S., Onoda, N., Noda, S., Asano, Y., Tauchi, Y., Morisaki, T., . . . Ohira, M. (2019). Sorafenib inhibits vascular endothelial cell proliferation stimulated by anaplastic thyroid cancer cells regardless of BRAF mutation status. *Int J Oncol, 55*(5), 1069-1076. doi:10.3892/ijo.2019.4881

➢ Jacob, F., & Monod, J. J. J. o. m. b. (1961). Genetic regulatory mechanisms in the synthesis of proteins. *3*(3), 318-356.

➢ Jadoun, S., Chauhan, N. P. S., Zarrintaj, P., Barani, M., Varma, R. S., Chinnam, S., & Rahdar, A. J. E. C. L. (2022). Synthesis of nanoparticles using microorganisms and their applications: a review. *20*(5), 3153-3197.

➢ Jain, L. (2009). Identification of Clinical, Laboratory and Genetic Covariates for Pharmacokinetics, Efficacy and Toxicity of Sorafenib in Patients with Solid Tumors.

➢ Jain, S. L. (2013). *Malignant: How cancer becomes us*: Univ of California Press.

➢ Janani, R., Harris, A. W., Strasser, A., Dhanoa, S., Plyam, R., Osmond, D. G. J. B. c. d., . . . ceUs, l. o. p. (1997). Effect of a bcl-2 transgene on production and localization of precursor B ceUs in mouse bone marrow. 73.

➢ Jeevanandam, J., Barhoum, A., Chan, Y. S., Dufresne, A., & Danquah, M. K. J. B. j. o. n. (2018). Review on nanoparticles and nanostructured materials: history, sources, toxicity and regulations. *9*(1), 1050-1074.

➢ Jemal, A., Bray, F., Center, M. M., Ferlay, J., Ward, E., & Forman, D. J. C. a. c. j. f. c. (2011). Global cancer statistics. *61*(2), 69-90.

➢ Jin, X., Demere, Z., Nair, K., Ali, A., Ferraro, G. B., Natoli, T., . . . Zhu, C. J. N. (2020). A metastasis map of human cancer cell lines. *588*(7837), 331-336.

➢ Jones, R. J., & McCormick, T. M. (2024). *Rogue Cells: A Conversation on the Myths and Mysteries of Cancer*: JHU Press.

➢ Jyoti, K., Singh, A. J. J. o. G. E., & Biotechnology. (2016). Green synthesis of nanostructured silver particles and their catalytic application in dye degradation. *14*(2), 311-317.

➢ Kartsogiannis, V., Ng, K. W. J. M., & endocrinology, c. (2004). Cell lines and primary cell cultures in the study of bone cell biology. *228*(1-2), 79-102.

➢ Kaseb, A. O., & Kulik, L. M. J. H. C.-F. O. (2013). Sorafenib in the Continuum of Care for Hepatocellular Carcinoma: Challenges in Defining Optimal Practice.

➢ Kashyap, C., Tikka, B., Sharma, S., Kumari, S., Verma, P., Sharma, S., & Arya, V. (2011). Human cancer cell lines-A brief communication. *Journal of chemical and phrmaceutical research, 3*, 514-520.

➢ Keating, G. M. (2017). Sorafenib: A Review in Hepatocellular Carcinoma. *Target Oncol, 12*(2), 243-253. doi:10.1007/s11523-017-0484-7

➢ Keijok, W. J., Pereira, R. H. A., Alvarez, L. A. C., Prado, A. R., da Silva, A. R., Ribeiro, J., . . . Guimarães, M. C. C. J. S. R. (2019). Controlled biosynthesis of gold nanoparticles with Coffea arabica using factorial design. *9*(1), 16019.

➢ Kelly, P. J., & Arnell, R. D. J. V. (2000). Magnetron sputtering: a review of recent developments and applications. *56*(3), 159-172.

➢ Khan, A., Fornes, O., Stigliani, A., Gheorghe, M., Castro-Mondragon, J. A., Van Der Lee, R., . . . Tan, G. J. N. a. r. (2018). JASPAR 2018: update of the open-access database of transcription factor binding profiles and its web framework. *46*(D1), D260-D266.

➢ Khan, A. U., Malik, N., Khan, M., Cho, M. H., Khan, M. M. J. B., & engineering, b. (2018). Fungi-assisted silver nanoparticle synthesis and their applications. *41*, 1-20.

➢ Khan, H., Yerramilli, A., D'Oliveira, A., Alford, T., Boffito, D., & Patience, G. (2020). Experimental methods in chemical engineering: X-ray diffraction spectroscopy—XRD. *The Canadian Journal of Chemical Engineering, 98*. doi:10.1002/cjce.23747

➢ Khan, S., & Hossain, M. K. (2022). Classification and properties of nanoparticles. In *Nanoparticle-based polymer composites* (pp. 15-54): Elsevier.

➢ King, W., Toler, K., & Woodell-May, J. J. B. r. i. (2018). Role of White Blood Cells in Blood-and Bone Marrow-Based Autologous Therapies. *2018*(1), 6510842.

➢ Klein, C. A. J. N. (2013). Selection and adaptation during metastatic cancer progression. *501*(7467), 365-372.

➢ Klijn, C., Durinck, S., Stawiski, E. W., Haverty, P. M., Jiang, Z., Liu, H., . . . Liu, J. J. N. b. (2015). A comprehensive transcriptional portrait of human cancer cell lines. *33*(3), 306-312.

➢ Komarneni, S. J. J. o. M. C. (1992). Nanocomposites. *2*(12), 1219-1230.

➢ Kowalczyk, W., Waliszczak, G., Jach, R., & Dulińska-Litewka, J. J. C. (2021). Steroid receptors in breast cancer: understanding of molecular function as a basis for effective therapy development. *13*(19), 4779.

➢ Kubota, Y. J. T. K. j. o. m. (2012). Tumor angiogenesis and anti-angiogenic therapy. *61*(2), 47-56.

➢ Kumari, M. (2020). Cancer notes. In.

➢ Lai, T., Yang, Y., & Ng, S. K. J. P. (2013). Advances in mammalian cell line development technologies for recombinant protein production. *6*(5), 579-603.

➢ Laurent, S., Forge, D., Port, M., Roch, A., Robic, C., Vander Elst, L., & Muller, R. N. J. C. r. (2008). Magnetic iron oxide nanoparticles: synthesis, stabilization, vectorization, physicochemical characterizations, and biological applications. *108*(6), 2064-2110.

➢ Leowattana, W., Leowattana, T., & Leowattana, P. J. W. J. o. G. (2023). Systemic treatment for unresectable hepatocellular carcinoma. *29*(10), 1551.

➢ Leuthner, T. C., & Meyer, J. N. J. C. e. h. r. (2021). Mitochondrial DNA mutagenesis: feature of and biomarker for environmental exposures and aging. 1-15.

➢ Lewandowska, A. M., Rudzki, M., Rudzki, S., Lewandowski, T., Laskowska, B. J. A. o. A., & Medicine, E. (2018). Environmental risk factors for cancer-review paper. *26*(1), 1-7.

➢ Lewis, W. D., Lilly, S., & Jones, K. L. J. A. f. p. (2020). Lymphoma: diagnosis and treatment. *101*(1), 34-41.

➢ Lind, S. E., DelVecchio Good, M., Seidel, S., Csordas, T., & Good, B. J. J. J. o. C. O. (1989). Telling the diagnosis of cancer. *7*(5), 583-589.

➢ Llames, S., García-Pérez, E., Meana, Á., Larcher, F., & Del Río, M. J. T. E. P. B. R. (2015). Feeder layer cell actions and applications. *21*(4), 345-353.

➢ Llovet, J., Ricci, S., Mazzaferro, V., Hilgard, P., Raoul, J., Zeuzem, S., . . . Bruix, J. J. J. o. c. o. (2007). Randomized phase III trial of sorafenib versus placebo in patients with advanced hepatocellular carcinoma (HCC). *25*(18_suppl), LBA1-LBA1.

➢ Lu, A. H., & Schüth, F. J. A. M. (2006). Nanocasting: a versatile strategy for creating nanostructured porous materials. *18*(14), 1793-1805.

➢ Lv, D., Hu, Z., Lu, L., Lu, H., & Xu, X. J. O. l. (2017). Three-dimensional cell culture: A powerful tool in tumor research and drug discovery. *14*(6), 6999-7010.

➢ Malhotra, S., & Sandhir, R. J. A. H. P. i. N. D. (2023). Insights into the neuroprotective strategies to alleviate neurodegenerative conditions: Role of Ayurvedic herbs and their bioactives. 113-140.

➢ Mazzoccoli, G., Miele, L., Oben, J., Grieco, A., & Vinciguerra, M. J. C. d. t. (2016). Biology, epidemiology, clinical aspects of hepatocellular carcinoma and the role of sorafenib. *17*(7), 783-799.

➢ McCormick, F. J. A. i. C. R. (2022). A brief history of RAS and the RAS Initiative. *153*, 1-27.

➢ McNamara, M. G., Slagter, A. E., Nuttall, C., Frizziero, M., Pihlak, R., Lamarca, A., . . . Knox, J. J. J. E. J. o. C. (2018). Sorafenib as first-line therapy in patients with advanced Child-Pugh B hepatocellular carcinoma—A meta-analysis. *105*, 1-9.

➢ Midgley, R. S., & Kerr, D. J. B. (2000). Adjuvant therapy. *321*(7270), 1208-1211.

➢ Mierzwa, M. L., Nyati, M. K., Morgan, M. A., & Lawrence, T. S. J. T. o. (2010). Recent advances in combined modality therapy. *15*(4), 372-381.

➢ Milevoj Kopcinovic, L., Culej, J., Jokic, A., Bozovic, M., & Kocijan, I. (2020). Laboratory testing of extravascular body fluids: National recommendations on behalf of the Croatian Society of Medical Biochemistry and Laboratory Medicine. Part I - Serous fluids. *Biochem Med (Zagreb), 30*(1), 010502. doi:10.11613/bm.2020.010502

➢ Miramontes, O., & Alvarez-Buylla, E. R. (2018). *Cancer: a complex disease*: CopIt ArXives.

➢ Momenimovahed, Z., Mazidimoradi, A., Maroofi, P., Allahqoli, L., Salehiniya, H., & Alkatout, I. J. C. r. (2023). Global, regional and national burden, incidence, and mortality of cervical cancer. *6*(3), e1756.

➢ Momtazi-Borojeni, A. A., Behbahani, M., & Sadeghi-Aliabadi, H. (2013). Antiproliferative activity and apoptosis induction of crude extract and fractions of avicennia marina. *Iran J Basic Med Sci, 16*(11), 1203-1208.

➢ Moran, T. C., Kaye, A. D., Mai, A. H., & Bok, L. R. J. R. (2013). Sedation, analgesia, and local anesthesia: a review for general and interventional radiologists. *33*(2), E47-E60.

➢ Mouradov, D., Sloggett, C., Jorissen, R. N., Love, C. G., Li, S., Burgess, A. W., . . . Wormald, S. J. C. r. (2014). Colorectal cancer cell lines are representative models of the main molecular subtypes of primary cancer. *74*(12), 3238-3247.

➢ Mundkinajeddu, D., & Agarwal, A. (2004). The need for establishing identities of 'bacoside A and B', the putative major bioactive saponins of Indian medicinal plant Bacopa monnieri. *Phytomedicine : international journal of phytotherapy and phytopharmacology, 11*, 264-268. doi:10.1078/0944-7113-00351

➢ Neto, L. J. V., Reverete, M., Junior, R. C. M., Machado, N. M., Joshi, R. K., dos Santos Buglio, D., . . . Tanaka, M. (2024). The Neuroprotective and Cognitive-Enhancing Effects of Bacopa monnieri: A Systematic Review.

➢ Ney, G. M., Yang, K. B., Ng, V., Liu, L., Zhao, M., Kuk, W., . . . Jones, M. A. J. C. r. (2021). Oncogenic N-Ras mitigates oxidative stress–induced apoptosis of hematopoietic stem cells. *81*(5), 1240-1251.

➢ Nikzamir, M., Akbarzadeh, A., Panahi, Y. J. J. o. D. D. S., & Technology. (2021). An overview on nanoparticles used in biomedicine and their cytotoxicity. *61*, 102316.

➢ Nojiri, K., Sugimoto, K., Shiraki, K., Tameda, M., Inagaki, Y., Ogura, S., . . . Yamamoto, N. J. I. j. o. o. (2013). Sorafenib and TRAIL have synergistic effect on hepatocellular carcinoma. *42*(1), 101-108.

➢ Odziomek, K., Ushizima, D., Oberbek, P., Kurzydłowski, K. J., Puzyn, T., & Haranczyk, M. (2016). Scanning electron microscopy image representativeness: Morphological data on nanoparticles. *Journal of Microscopy, 265*. doi:10.1111/jmi.12461

➢ Ogle, L. F. (2017). *Exploring circulating biomarkers in patients with hepatocellular cancer.* Newcastle University,

➢ Panigrahi, S., Kundu, S., Ghosh, S., Nath, S., & Pal, T. J. J. o. n. R. (2004). General method of synthesis for metal nanoparticles. *6*(4), 411-414.

➢ Pantidos, N., Horsfall, L. E. J. J. o. N., & Nanotechnology. (2014). Biological synthesis of metallic nanoparticles by bacteria, fungi and plants. *5*(5), 1.

➢ Papageorgiou, D. G., Kinloch, I. A., & Young, R. J. J. P. i. m. s. (2017). Mechanical properties of graphene and graphene-based nanocomposites. *90*, 75-127.

➢ Pelcovits, A., & Niroula, R. J. R. I. m. j. (2020). Acute myeloid leukemia: a review. *103*(3), 38-40.

➢ Petkovich, N. D., & Stein, A. J. C. S. R. (2013). Controlling macro-and mesostructures with hierarchical porosity through combined hard and soft templating. *42*(9), 3721-3739.

➢ Pinkerton, J. V. J. N. E. J. o. M. (2020). Hormone therapy for postmenopausal women. *382*(5), 446-455.

➢ PR Xavier, C., Pesic, M., & Helena Vasconcelos, M. J. C. c. d. t. (2016). Understanding cancer drug resistance by developing and studying resistant cell line models. *16*(3), 226-237.

➢ Prabhuji, S. K., Rao, G. P., Pande, S., Srivastava, G. K., Srivastava, C., Srivastava, A. K. J. M. P.-I. J. o. P., & Industries, R. (2023). Bacopa monnieri (L.) Wettst.: A potential medicinal herb called 'Brahmi'. *15*(1), 1-12.

➢ Pujol, P., Barberis, M., Beer, P., Friedman, E., Piulats, J. M., Capoluongo, E. D., . . . Foulkes, W. D. J. E. J. o. C. (2021). Clinical practice guidelines for BRCA1 and BRCA2 genetic testing. *146*, 30-47.

➢ Raab, S. S., & Grzybicki, D. M. J. C. a. c. j. f. c. (2010). Quality in cancer diagnosis. *60*(3), 139-165.

➢ Raju, M. I. (2022). *Arresting tumor cell proliferation and inhibition of AKT pathway via the use of multikinase inhibitor sorafenib forthe treatment of glioblastoma.* Brac University,

➢ Ramesh, K. T., & Ramesh, K. (2009). *Nanomaterials*: Springer.

➢ Rashid, H. U., Yu, K., Umar, M. N., Anjum, M. N., Khan, K., Ahmad, N., & Jan, M. T. J. R. A. M. S. (2015). Catalyst role in chemical vapor deposition (CVD) process: a review. *40*(3), 235-248.

➢ Richter, M., Piwocka, O., Musielak, M., Piotrowski, I., Suchorska, W. M., Trzeciak, T. J. F. i. C., & Biology, D. (2021). From donor to the lab: a fascinating journey of primary cell lines. *9*, 711381.

➢ Rinke, M., & Ruehl-Fehlert, C. (2024). Bone, Cartilage, Muscle, Tooth. In *Toxicologic Pathology* (pp. 192-241): CRC Press.

➢ Russell, P. J., Kingsley, E. A. J. P. c. m., & protocols. (2003). Human prostate cancer cell lines. 21-39.

➢ Russo, A., Borrelli, F., Campisi, A., Acquaviva, R., Raciti, G., & Vanella, A. J. L. s. (2003). Nitric oxide-related toxicity in cultured astrocytes: effect of Bacopa monniera. *73*(12), 1517-1526.

➢ Sadaqat, M., Qasim, M., ul Qamar, M. T., Masoud, M. S., Ashfaq, U. A., Noor, F., . . . medicine. (2023). Advanced network pharmacology study reveals multi-pathway and multi-gene regulatory molecular mechanism of Bacopa monnieri in liver cancer based on data mining, molecular modeling, and microarray data analysis. *161*, 107059.

➢ Saied, I., & MsHAMsUDDIN, A. J. A. R. (1998). In HepG2 human liver cancer cell line. *18*, 4083-4090.

➢ Santoro, M., Moccia, M., Federico, G., & Carlomagno, F. J. G. (2020). RET gene fusions in malignancies of the thyroid and other tissues. *11*(4), 424.

➢ Sarkar, S., Horn, G., Moulton, K., Oza, A., Byler, S., Kokolus, S., & Longacre, M. J. I. j. o. m. s. (2013). Cancer development, progression, and therapy: an epigenetic overview. *14*(10), 21087-21113.

➢ Schwartz, S. M. J. C. C. (2024). Epidemiology of cancer. *70*(1), 140-149.

➢ Sedeky, A. S., Khalil, I. A., Hefnawy, A., & El-Sherbiny, I. M. J. E. J. o. P. S. (2018). Development of core-shell nanocarrier system for augmenting piperine cytotoxic activity against human brain cancer cell line. *118*, 103-112.

➢ Sekhar, V. C., Viswanathan, G., & Baby, S. (2019). Insights Into the Molecular Aspects of Neuroprotective Bacoside A and Bacopaside I. *Curr Neuropharmacol, 17*(5), 438-446. doi:10.2174/1570159x16666180419123022

➢ Shah, M., Fawcett, D., Sharma, S., Tripathy, S. K., & Poinern, G. E. J. J. M. (2015). Green synthesis of metallic nanoparticles via biological entities. *8*(11), 7278-7308.

➢ Sigmund, P. J. P. r. (1969). Theory of sputtering. I. Sputtering yield of amorphous and polycrystalline targets. *184*(2), 383.

➢ Simpson, T., Pase, M., Stough, C. J. E. B. C., & Medicine, A. (2015). Bacopa monnieri as an antioxidant therapy to reduce oxidative stress in the aging brain. *2015*(1), 615384.

➢ Singh, B., Singh, J. P., Kaur, A., & Singh, N. J. F. c. (2016). Bioactive compounds in banana and their associated health benefits–A review. *206*, 1-11.

➢ Singh, V., Yadav, P., & Mishra, V. J. G. s. o. n. f. b. a. (2020). Recent advances on classification, properties, synthesis, and characterization of nanomaterials. 83-97.

➢ Sivakumari, K., Janani, P., Rajesh, S. J. H. o. A. M., & Research, i. U. i. C. (2022). DEN-induced hepatocellular carcinoma in animal model. 1-23.

➢ Song, S., Wang, C., Wang, S., Siegel, R. A., & Sun, C. C. J. I. j. o. p. (2021). Efficient development of sorafenib tablets with improved oral bioavailability enabled by coprecipitated amorphous solid dispersion. *610*, 121216.

➢ Subrahmanyam, K., Panchakarla, L., Govindaraj, A., & Rao, C. J. T. J. o. P. C. C. (2009). Simple method of preparing graphene flakes by an arc-discharge method. *113*(11), 4257-4259.

➢ Sukumaran, N. P., Amalraj, A., & Gopi, S. J. C. t. i. m. (2019). Neuropharmacological and cognitive effects of Bacopa monnieri (L.) Wettst–A review on its mechanistic aspects. *44*, 68-82.

➢ Summers, M. C., & Biggers, J. D. J. H. r. u. (2003). Chemically defined media and the culture of mammalian preimplantation embryos: historical perspective and current issues. *9*(6), 557-582.

➢ Sun, X., Bandara, N. J. T. i. F. S., & Technology. (2019). Applications of reverse micelles technique in food science: A comprehensive review. *91*, 106-115.

➢ Tahir, U., Shim, Y. B., Kamran, M. A., Kim, D.-I., Jeong, M. Y. J. J. o. N., & Nanotechnology. (2021). Nanofabrication techniques: challenges and future prospects. *21*(10), 4981-5013.

➢ Talapin, D. V., & Shevchenko, E. V. J. C. R. (2016). Introduction: nanoparticle chemistry. *116*(18), 10343-10345.

➢ Talukder, M., Bi, S.-S., Jin, H.-T., Ge, J., Zhang, C., Lv, M.-W., & Li, J.-L. J. E. P. (2021). Cadmium induced cerebral toxicity via modulating MTF1-MTs regulatory axis. *285*, 117083.

➢ Tamura, R. J. I. j. o. m. s. (2021). Current understanding of neurofibromatosis type 1, 2, and schwannomatosis. *22*(11), 5850.

➢ Tan, S., Li, D., Zhu, X. J. B., & Pharmacotherapy. (2020). Cancer immunotherapy: Pros, cons and beyond. *124*, 109821.

➢ Tang, W., Chen, Z., Zhang, W., Cheng, Y., Zhang, B., Wu, F., . . . therapy, t. (2020). The mechanisms of sorafenib resistance in hepatocellular carcinoma: theoretical basis and therapeutic aspects. *5*(1), 87.

➢ Tarin, D. (2011). *Cell and tissue interactions in carcinogenesis and metastasis and their clinical significance.* Paper presented at the Seminars in cancer biology.

➢ Testa, U., Castelli, G., & Pelosi, E. J. C. (2018). Lung cancers: molecular characterization, clonal heterogeneity and evolution, and cancer stem cells. *10*(8), 248.

➢ Tewari, M. (2022). CANCER AND ITS TREATMENT: AN OVERVIEW. *International Journal of Advanced Research, 10*, 950-956. doi:10.21474/IJAR01/14476

➢ Thakkar, K. N., Mhatre, S. S., Parikh, R. Y. J. N. n., biology, & medicine. (2010). Biological synthesis of metallic nanoparticles. *6*(2), 257-262.

➢ Thiruvengadathan, R., Korampally, V., Ghosh, A., Chanda, N., Gangopadhyay, K., & Gangopadhyay, S. J. R. o. P. i. P. (2013). Nanomaterial processing using self-assembly-bottom-up chemical and biological approaches. *76*(6), 066501.

➢ Thomas-Schoemann, A., Blanchet, B., Bardin, C., Noé, G., Boudou-Rouquette, P., Vidal, M., & Goldwasser, F. J. C. r. i. o. h. (2014). Drug interactions with solid tumour-targeted therapies. *89*(1), 179-196.

➢ Thompson, L. F. (1983). An introduction to lithography. In: ACS Publications.

➢ Tlemsani, C., Huillard, O., Arrondeau, J., Boudou-Rouquette, P., Cessot, A., Blanchet, B., . . . toxicology. (2015). Effect of glucuronidation on transport and tissue accumulation of tyrosine kinase inhibitors: consequences for the clinical management of sorafenib and regorafenib. *11*(5), 785-794.

➢ Trimble, E., Ungerleider, R., Abrams, J., Kaplan, R., Feigal, E., Smith, M., . . . Friedman, M. J. C. (1993). Neoadjuvant therapy in cancer treatment. *72*(S11), 3515-3524.

➢ Trusolino, L., Bertotti, A., & Comoglio, P. M. J. N. r. M. c. b. (2010). MET signalling: principles and functions in development, organ regeneration and cancer. *11*(12), 834-848.

➢ Tuccitto, A. (2018). *pH Regulatory Molecules In The Tumour Microenvironment: Modulators Of Aggressiveness And Immune Profile Of Human Hepatocellular Carcinoma*: Open University (United Kingdom).

➢ Valotto Neto, L. J., Reverete de Araujo, M., Moretti Junior, R. C., Mendes Machado, N., Joshi, R. K., dos Santos Buglio, D., . . . Tanaka, M. J. A. (2024). Investigating the Neuroprotective and Cognitive-Enhancing Effects of Bacopa monnieri: A Systematic Review Focused on Inflammation, Oxidative Stress, Mitochondrial Dysfunction, and Apoptosis. *13*(4), 393.

➢ Vineis, P., Schatzkin, A., & Potter, J. D. J. C. (2010). Models of carcinogenesis: an overview. *31*(10), 1703-1709.

➢ Vishnupriya, P., & Padma, V. V. J. R. O. S. (2017). A review on the antioxidant and therapeutic potential of Bacopa monnieri. *3*, 111-120.

➢ Walsh, N. M., & Cerroni, L. J. J. o. C. P. (2021). Merkel cell carcinoma: A review. *48*(3), 411-421.

➢ Walter, L. C., & Covinsky, K. E. J. J. (2001). Cancer screening in elderly patients: a framework for individualized decision making. *285*(21), 2750-2756.

➢ Wang, L., Chen, M., Ran, X., Tang, H., & Cao, D. J. P. (2023). Sorafenib-based drug delivery systems: applications and perspectives. *15*(12), 2638.

➢ Weinberg, R. A. J. S. A. (1996). How cancer arises. *275*(3), 62-70.

➢ Wilding, J. L., & Bodmer, W. F. J. C. r. (2014). Cancer cell lines for drug discovery and development. *74*(9), 2377-2384.

➢ Wohlleben, W., Punckt, C., Aghassi-Hagmann, J., Siebers, F., Menzel, F., Esken, D., . . . Innovations, I. (2017). Nanoenabled products: categories, manufacture, and applications. 409-464.

➢ Yadav, A. R., & Mohite, S. K. J. A. J. o. P. R. (2020). Cancer-A silent killer: An overview. *10*(3), 213-216.

➢ Yang, Z., Zhang, Y., & Schnepp, Z. J. J. o. M. C. A. (2015). Soft and hard templating of graphitic carbon nitride. *3*(27), 14081-14092.

➢ Yasmin, I., Khan, W. A., Naz, S., Iqbal, M. W., Awuchi, C. G., Egbuna, C., . . . Diabetes. (2021). Etiology of obesity, cancer, and diabetes. 1-27.

➢ Yen, T., Stanich, P. P., Axell, L., & Patel, S. G. (2022). APC-associated polyposis conditions.

➢ Yuliarto, B., Zulhendry, D. W., Septiani, N. L. W., Irzaman, I., Ferdiansjah, F., Fahmi, M. Z., & Nugraha, N. (2019). *Synthesis and Characterization of Tin Oxide-MultiWalled Carbon Nanotube Composite Material as Carbon Monoxide Gas Sensor.* Paper presented at the Materials Science Forum.

➢ Yun, N. L. T. (2017). *Effect of peroxisome proliferator-activated receptor polymorphism in relation to alcohol metabolism and oestrogen levels, and their association with breast cancer.* Itä-Suomen yliopisto,

➢ Zhang, D. J. P. i. M. S. (2004). Processing of advanced materials using high-energy mechanical milling. *49*(3-4), 537-560.

➢ Zhang, Y., Peng, P., Liu, C., Xu, Y., & Zhang, H. J. J. o. I. M. (2022). A sequential resampling approach for imbalanced batch process fault detection in semiconductor manufacturing. 1-16.

➢ Zhang, Y., Zhang, L., & Zhou, C. J. A. o. c. r. (2013). Review of chemical vapor deposition of graphene and related applications. *46*(10), 2329-2339.

➢ Zugazagoitia, J., Guedes, C., Ponce, S., Ferrer, I., Molina-Pinelo, S., & Paz-Ares, L. J. C. t. (2016). Current challenges in cancer treatment. *38*(7), 1551-1566.